Supporting Information for:

A Tetranuclear Nickel Cluster Isolated in Multiple High-Valent States

Samuel I. Jacob,[a] Iskander Douair,[b] Guang Wu,[a] Laurent Maron,[b] and Gabriel Ménard*[a]

[a]Department of Chemistry and Biochemistry, University of California, Santa Barbara, California 93106, United States
[b]CNRS, INSA, UPS, UMR 5215, LPCNO, University de Toulouse, 135 avenue de Rangueil, 31077 Toulouse, France

Table of Contents

1) Methods:

Techniques and Reagents. All manipulations were performed under an atmosphere of dry N_2 by means of standard Schlenk or glovebox techniques (MBRAUN UNIlab Pro SP Eco equipped with a −40 °C freezer), unless stated otherwise. Hexanes and DCM (Fisher) were dried using an MBRAUN-Solvent Purification System and stored over activated 4 Å molecular sieves for 2 days prior to use. 1,1,2,2-Tetrachloroethane (TCE; Fisher) was degassed over 4 freeze-pump-thaw cycles and stored over 4 Å molecular sieves for 2 days prior to use. $Ni(OAc)_2•4H_2O$, Acetone, Acetonitrile, and $[NO][PF_6]$ were all purchased from Fisher and used as received. Deuterated solvents were purchased from Cambridge Isotope Laboratories, then degassed, and stored over 4 Å molecular sieves for at least 2 days prior to use. Celite was dried by heating above 250 °C under dynamic vacuum for at least 48 h prior to use. 5,5'-(9,9-Dimethylxanthene-4,5-diyl)bis(salicylaldehyde)[1] and $[(2,4\text{-}C_6H_3Br_2)_3N][B(C_6F_5)_4]$[2] were prepared according to literature procedures.

Spectroscopic Measurements. NMR spectra were obtained on Agilent Technologies 400 and 600 MHz spectrometers, and referenced to residual solvent or externally (^{19}F, $CFCl_3$). Chemical shifts (δ) are recorded in ppm, and the coupling constants are in Hz. Elemental analyses (C, H, N) were recorded at the University of California, Berkeley using a PerkinElmer 2400 Series II combustion analyzer. UV−vis−NIR spectroscopy was performed using a Perkin Elmer Lambda 750 UV/VIS spectrometer with 1 mm quartz cuvettes with a teflon seal and 1 cm IR quartz cuvettes with a screwcap top. Perpendicular-mode X-band EPR spectra were collected on a Bruker EMX EPR Spectrometer equipped with an Oxford ESR 900 liquid nitrogen cryostat. Data acquisition was collected at 100K in frozen DCM. EPR data was simulated using the program PHI.[3]

Magnetic Measurements. Solution magnetic moment determinations were performed by the Evans method using 1,2-difluorobenzene as residual solvent.[4] Solid-state magnetic measurements were collected using a Quantum Design MPMS SQUID magnetometer in the RSO mode. The sample was prepared in the glovebox. Magnetic susceptibility data was corrected for diamagnetism of the sample, estimated using Pascal's constants.[5] $\chi_M T$ data was fit using the exchange Hamiltonian, $\hat{H}_{ex} = -2\sum_{i=1}^{ns-1}\sum_{j=i+1}^{ns} J_{ij}\, S_i S_j$, where J_{ij} are the exchange coupling constants of spins i and j, and ns is the number of spins. SQUID data was fit using the program PHI.[3]

Electrochemical Measurements. Cyclic voltammetry was performed on a CH Instruments 630E electrochemical analysis potentiostat, equipped with a 3 mm diameter glassy carbon working electrode, a Ag wire pseudo-reference electrode, and a Pt wire counter electrode in a conventional three-electrode cell. TCE was used as the solvent for electrochemical measurements with $[Bu_4N][PF_6]$ (0.1 M) as the supporting electrolyte. The glassy carbon working electrode was cleaned prior to each experiment by polishing with 1, 0.3, and 0.05 mm alumina (CH Instruments) in descending order, followed by a water and acetone solvent rinse and finally sonication in acetone for 2 min. The potential of the pseudo-reference was referenced to the Fc/Fc^+ redox couple.

2) Synthesis:

LH_4. A 50 mL round bottom flask was charged with 5,5'-(9,9-Dimethylxanthene-4,5-diyl)bis(salicylaldehyde)[1] (400 mg, 0.8879 mmol), *o*-phenylenediamine (960.2 mg, 8.879 mmol), and ethanol (25 mL). The reaction was refluxed for 4 hours open to atmosphere. After a few minutes the reactants went into solution and formed a deep orange color. Eventually, yellow precipitates were formed. After reflux, the reaction was allowed to cool to room temperature and was filtered. The yellow product was washed with 200 mL of ethanol and dried under vacuum. Yield: 470 mg (83.9%). NMR: ^{1}H NMR (400 MHz, $CDCl_3$): δ 13.28 (s, 2H, OH), 8.05 (s, 2H, HC=N), 7.43 (dd, *J* = 8 Hz, 4 Hz, 2H), 7.23 (dd, *J* = 12 Hz, 4 Hz, 2H), 7.17-7.06 (m, 8H), 6.86-6.79 (m, 8H), 4.51 (s, 4H, NH), 1.74 (s, 6H, Me). ^{13}C{^{1}H} NMR (101 MHz, $(CD_3)_2CO$): δ 162.47, 160.38, 148.18, 143.32, 135.73, 135.39, 133.49, 131.61, 130.16, 129.16, 128.90, 128.69, 126.00, 124.08, 120.03, 119.34, 118.18, 116.94, 116.39, 35.40, 32.35. MS (ESI(+), MeCN) *m/z*: $[M + H]^+$ 631.3.

L_2Ni_4 ($[Ni_4]$). To a 50 mL round bottom flask was added a magnetic stir bar, **LH_4** (592 mg, 0.9386 mmol), $Ni(OAc)_2$•$4H_2O$ (477 mg, 1.9169 mmol), and 25 mL of ethanol. The reaction was refluxed for 5 hrs. Upon heating, the powders went into solution and the color changed into a deep red where red precipitates eventually form. After reflux, the reaction was removed from heat and allowed to cool to room temperature. The reaction was filtered over a fine frit. The red solids were washed with ethanol until the washings were colorless. Next the crude product was washed with water (2 x 10 mL), acetone (5 x 10 mL), and acetonitrile (5 x 10 mL). The red product was dried under high vacuum at 100 °C overnight before bringing into the glovebox. Yield: 349.1 mg (50%). X-ray quality crystals were grown by vapor diffusion of hexanes into a concentrated DCM solution of the product at room temperature. NMR. ^{1}H NMR (600 MHz, $CDCl_3$): δ. 8.80 (d, *J* = 6 Hz, 4H), 7.44-7.38 (m, 8H), 7.33 (s, 4H), 7.29 (s, 4H), 7.26-7.20 (m, 12H), 7.18-7.08 (m, 8H), 6.48 (d, *J* = 12, 4H), 1.75 (s, 12H), 1.40 (s, 4H, NH). ^{13}C{^{1}H} NMR (101 MHz, $(CD_3)_2CO$): δ 162.26, 152.02, 150.73, 147.09, 145.08, 136.47, 134.56, 130.49, 129.53, 128.19, 127.70, 127.43, 125.10, 123.77, 123.39, 121.64, 114.70, 34.67, 33.19, 30.16, 25.59. UV-vis [DCM, λ_{max}/nm, (ε/M^{-1} cm^{-1})]: 451 (20,779), 384 (50,754), 318 (94,775), 287 (98,306), 256 (105,915). MS (MALDI) *m/z*: 1484.342. Anal. Calcd. for $C_{82}H_{60}N_8Ni_4O_6$: C, 66.18; H, 4.06; N, 7.53. Found: C, 66.34; H, 3.83; N, 7.14.

$[L_2Ni_4][PF_6]$ ($[Ni_4]^+$). In the glovebox, a 20 mL scintillation vial was charged with 1 equiv of **$[Ni_4]$** (50.5 mg, 0.0339 mmol) and 2 mL of DCM. The slurry was frozen in the glovebox coldwell. To the frozen slurry was added 0.9 equiv of $NOPF_6$ (5.3 mg, 0.0303 mmol) slurried in 1 mL of DCM. The reaction vial was placed back in the coldwell to freeze again. The frozen reaction was placed on the stir plate to thaw and stirred at glovebox temperature for 4 hours at which point the reaction color had turned brown. The reaction was dried under vacuum. The reaction vial was washed with benzene over a celite plug eluting a red solution of unreacted **$[Ni_4]$**. Once the benzene washes were colorless, the plug was washed with DCM until the washings were colorless. The DCM was removed under vacuum to provide **$[Ni_4]^+$**. X-ray quality crystals were grown by vapor diffusion of hexanes over a concentrated DCM solution of the product in a -40 °C freezer. Yield: 46.4 mg (93.7 %). NMR. ^{1}H NMR (400 MHz, CD_2Cl_2) Note: resonances are broadened and paramagnetically shifted and integrations are therefore not assigned: δ 16.66 (s), 10.76 (d, *J* = 8 Hz), 10.12 (s), 8.73 (t, *J* = 8 Hz), 7.02 (d, *J* = 8 Hz), 4.70 (s), 3.85 (s), 3.21 (d, *J* = 8 Hz), 2.65 (d, *J* = 8 Hz), 1.86 (s), -4.69 (s), -10.85 (s). ^{19}F NMR (376 MHz, CD_2Cl_2): δ -72.17 (d, J = 707.1 Hz). ^{31}P NMR (162 MHz, CD_2Cl_2): Silent. UV-Vis-NIR [DCM, λ_{max}/nm, (ε/M^{-1} cm^{-1})]: 1,300 (3,277), 436 sh (20,874), 363 (48,683), 306 (92,419), 278 sh (98,565) 260 (107,499). Anal. Calcd. for $C_{82}H_{60}F_6N_8Ni_4O_6P$•$CH_2Cl_2$: C, 58.02; H, 3.64; N, 6.52. Found: C, 57.88; H, 3.62; N, 6.23.

$[L_2Ni_4][B(C_6F_5)_4]_2$ ($[Ni_4]^{2+}$). In the glovebox, a 20 mL scintillation vial was charged with **$[Ni_4]$** (50.6 mg, 0.0340 mmol) and 3 mL of DCM. The slurry was frozen in the glovebox coldwell. $[(2,4\text{-}Br_2C_6H_3)_3N][B(C_6F_5)_4]$ (95.2 mg, 0.0681 mmol) was added to the frozen slurry along with 1 mL of DCM to aid with the transfer. The reaction vial was placed back in the Coldwell to freeze again. Once

frozen, the reaction was placed on the stir plate to thaw and stirred at glovebox temperature for 15 minutes. The reaction color turned dark brown. The solution was concentrated to 2 mL under vacuum and the product was crashed out of solution with 10 mL of hexanes and filtered over a celite plug. The plug was washed with 15 mL of benzene followed by 5 mL of hexanes. The product was eluted with DCM and dried under vacuum to yield 90.1 mg (93.1 %). X-ray quality crystals were grown by layering a concentrated DCM solution with hexanes in a -40 °C freezer. NMR. ^{1}H NMR (400 MHz, CD_2Cl_2) Note: resonances are broadened and paramagnetically shifted and integrations are therefore not assigned: δ 35.59, 21.09 7.87, 6.64 br, 4.21, 2.21, 1.80, -3.47, -15.32, -29.84, -80.66 br. ^{19}F NMR (376 MHz, CD_2Cl_2): δ 132.89 (bs, 16F), 163.01 (t, J = 18.8 Hz, 8F) , 166.70 (bs, 16F). UV-Vis-NIR [DCM, λ_{max}/nm, (ε/M^{-1} cm^{-1})]: 1410 (14,514), 778 (5,046), 542 sh (7,313), 454 (22,093), 352 (61,381), 294 sh (88,237), 260 (107,624). Anal. Calcd. for $C_{130}H_{60}B_2F_{40}N_8Ni_4O_6$: C, 54.86; H, 2.12; N, 3.94. Found: C, 54.89; H, 2.4; N, 4.08.

$[L_2Ni_4][B(C_6F_5)_4]_4$ ($[Ni_4]^{4+}$). In the glovebox, a 20 mL scintillation vial was charged with **$[Ni_4]$** (32 mg, 0.0215 mmol) and 3 mL of DCM. The slurry was frozen in the glovebox coldwell. To the frozen slurry was added $[(2,4\text{-}C_6H_3Br_2)_3N][B(C_6F_5)_4]$ (292 mg, 0.2089 mmol) of as a solid and 1 mL of DCM was used to help transfer residual powder. The reaction vial was placed back in the coldwell to freeze. The frozen reaction was placed on the stir plate to thaw and stirred at glovebox temperature for 5 minutes. The solution color turned black. The solvent was removed under vacuum. The crude product was washed with benzene over a celite plug until the washings were colorless (~30 mL). Once the washings were colorless, the plug was washed with another 10 mL of benzene to ensure removal of the $N(2,4\text{-}C_6H_3Br_2)_3$ byproduct. The plug was subsequently washed with 5 mL of hexanes. The product was eluted with DCM and dried under vacuum to yield 77.3 mg (85.5%). X-ray quality crystals were grown by layering a concentrated DCM solution of the product with hexanes in a -40 °C freezer. NMR. ^{1}H NMR (400 MHz, CD_2Cl_2) Note: resonances are broadened and paramagnetically shifted and integrations are therefore not assigned: δ 18.25 br, 16.49 br, 14.36, 12.91, 10.26, 9.76, 8.08, 4.86, 4.21, 4.10, 3.00, 2.68, 2.00, 1.91, 1.89, 1.87, 1.85, 1.84, 1.74, 1.72, 1.43, -2.31, -3.61, -13.02 br, -15.59 br, -35.53 br. ^{19}F NMR (376 MHz, CD_2Cl_2): δ 132.58 (bs, 32F), 162.7 (bs, 16F), 165.82 (bs, 32F). Vis-NIR [DCM, λ_{max}/nm, (ε/M^{-1} cm^{-1})]: 1,468 (22,099), 1662 sh (20,751).

3) NMR Spectroscopy

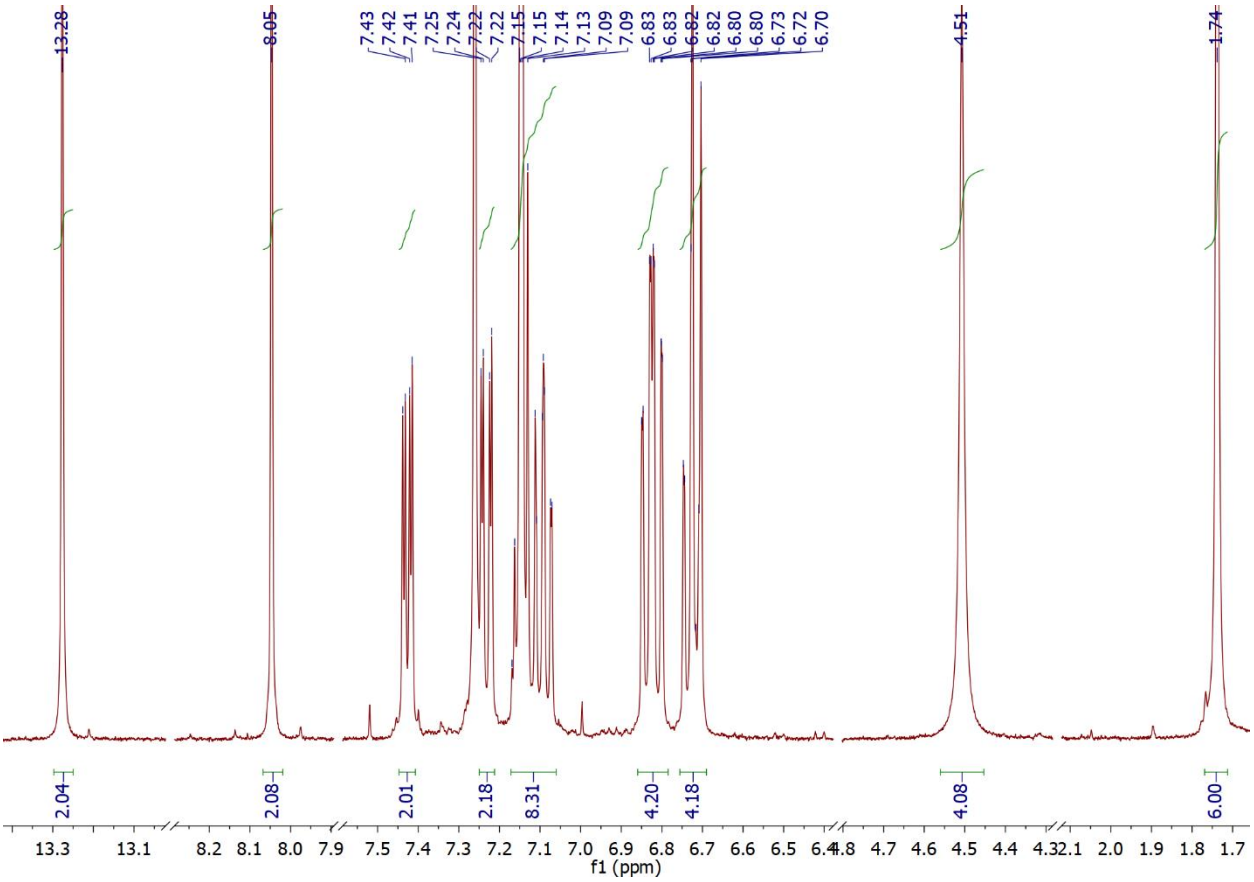

Figure S1. ^{1}H NMR (400 MHz) spectrum of **LH_4** in $CDCl_3$.

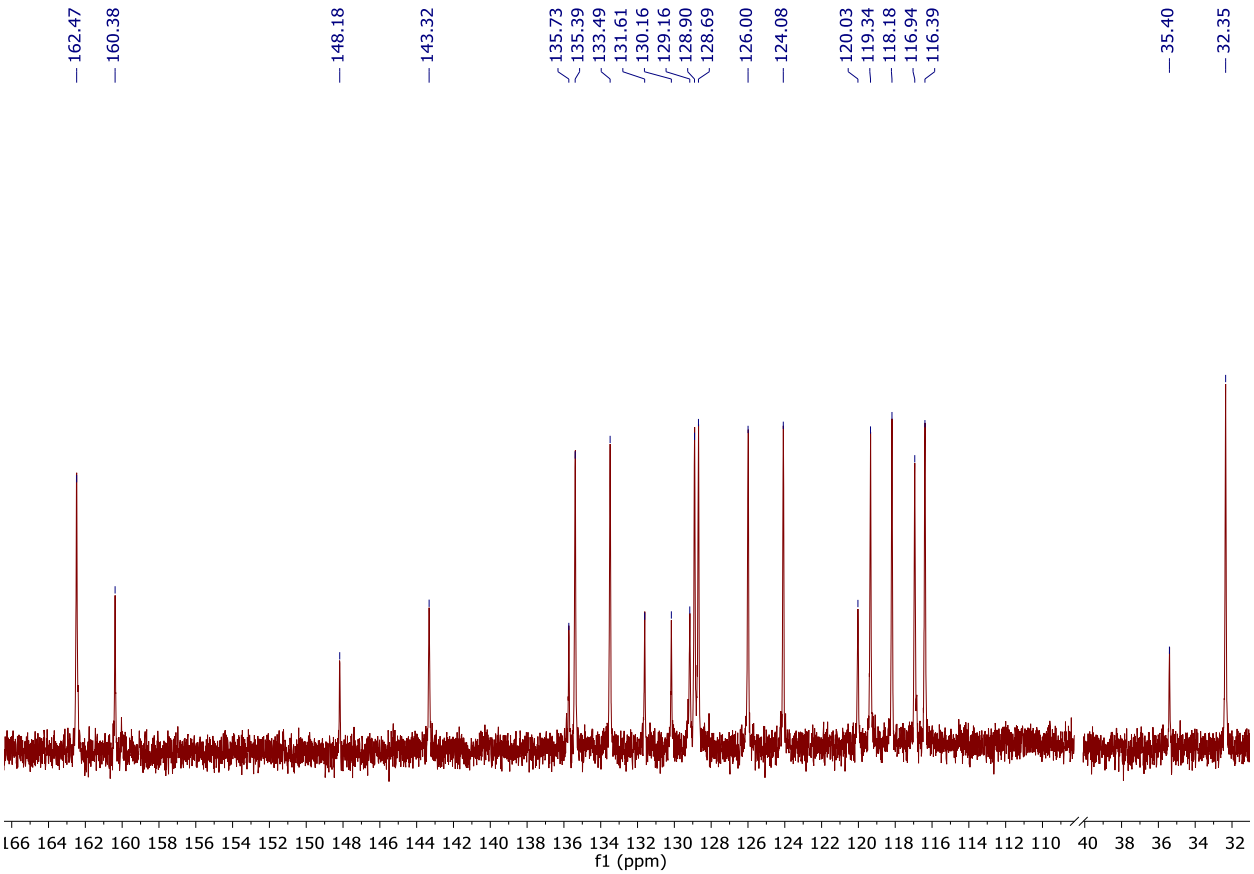

Figure S2. ^{13}C NMR (101 MHz) spectrum of **LH$_4$** in $(CD_3)_2CO$.

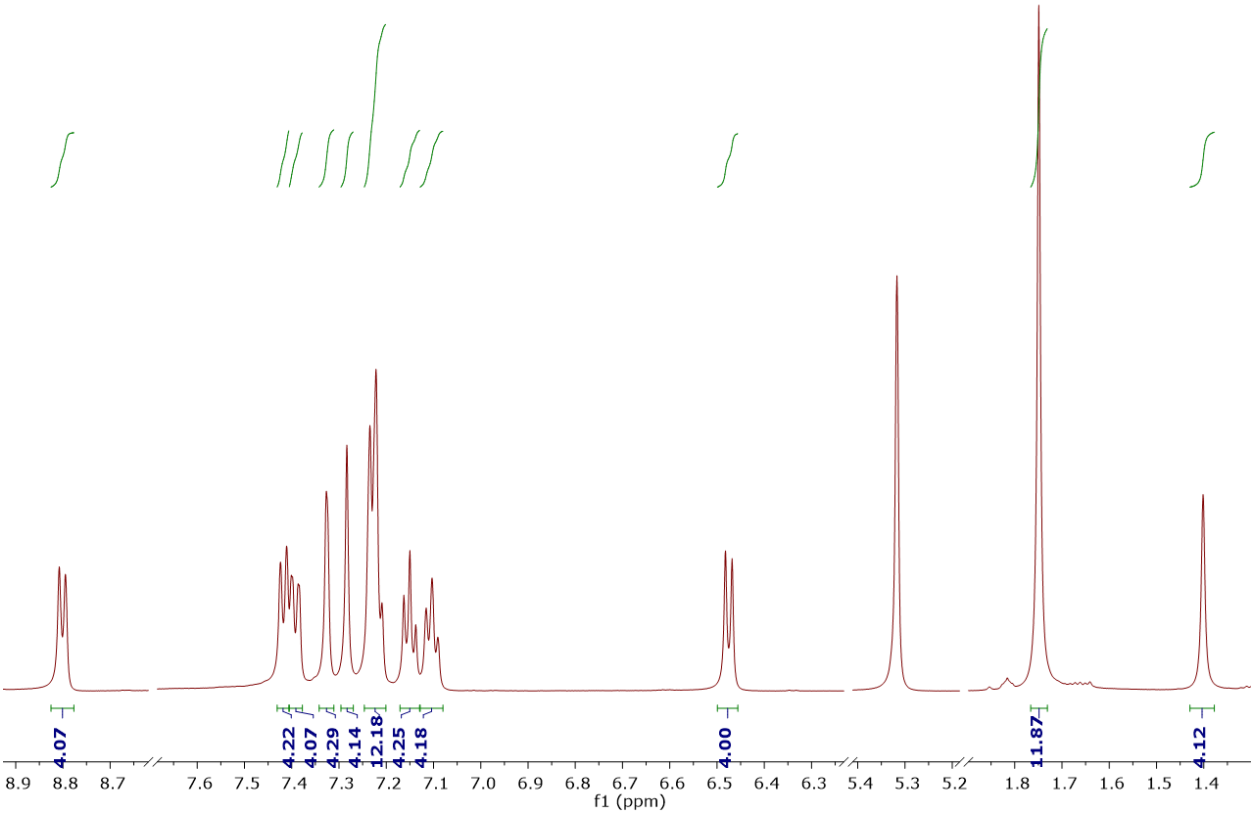

Figure S3. ^{1}H NMR (600 MHz) spectrum of **[Ni$_4$]** in CD_2Cl_2.

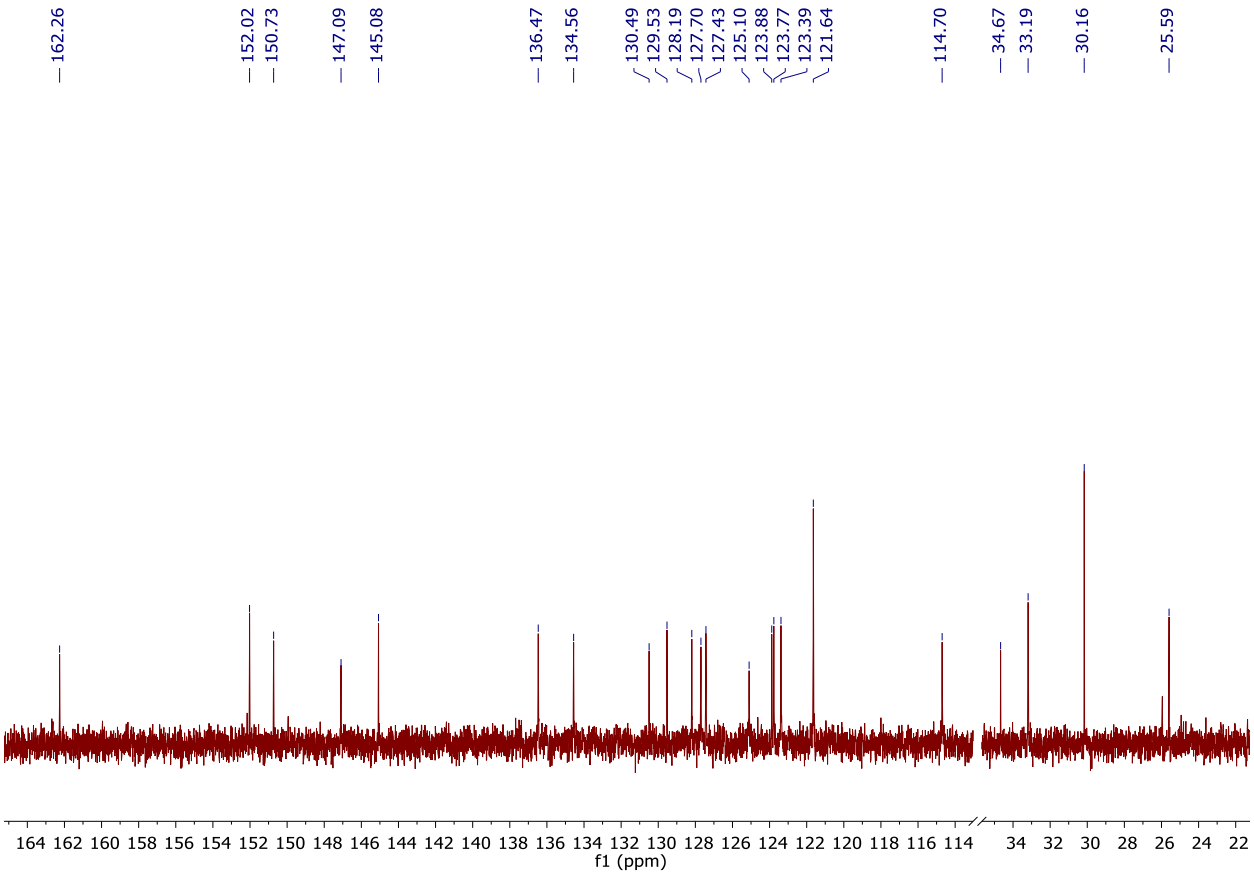

Figure S4. ^{13}C NMR (101 MHz) spectrum of **[Ni$_4$]** in CD_2Cl_2.

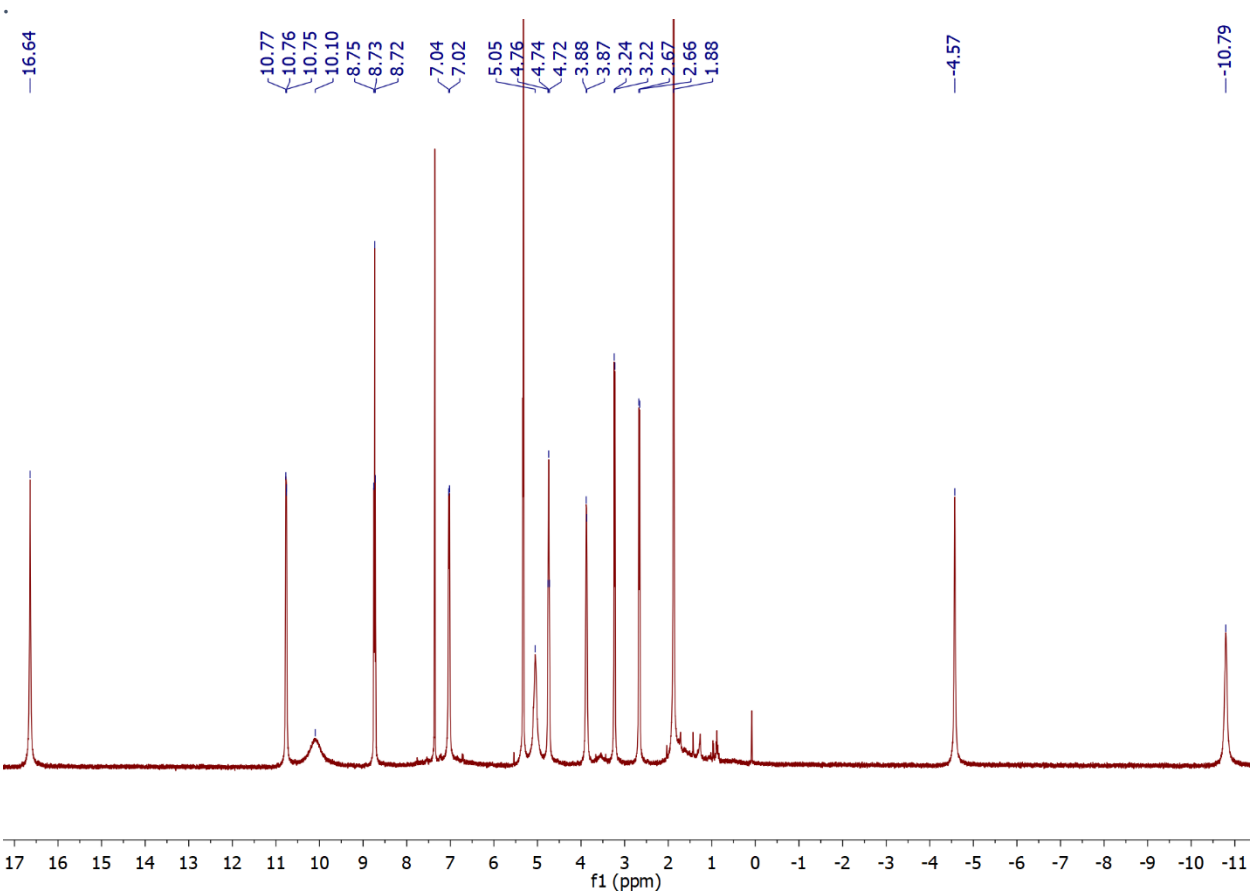

Figure S5. ^{1}H NMR (400 MHz) of **[Ni$_4$]$^+$** in CD_2Cl_2.

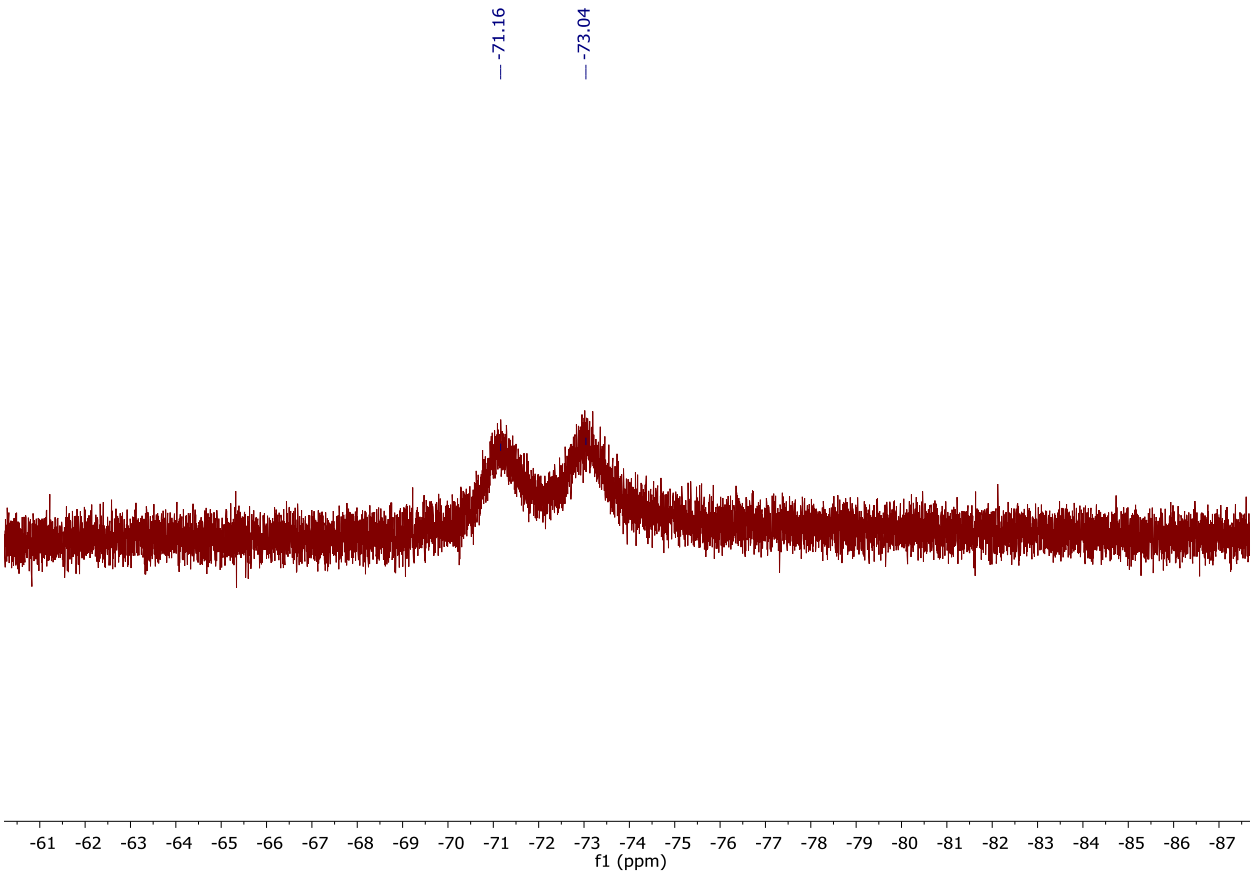

Figure S6. ^{19}F NMR (376 MHz) of **[Ni$_4$]**$^+$ in CD_2Cl_2.

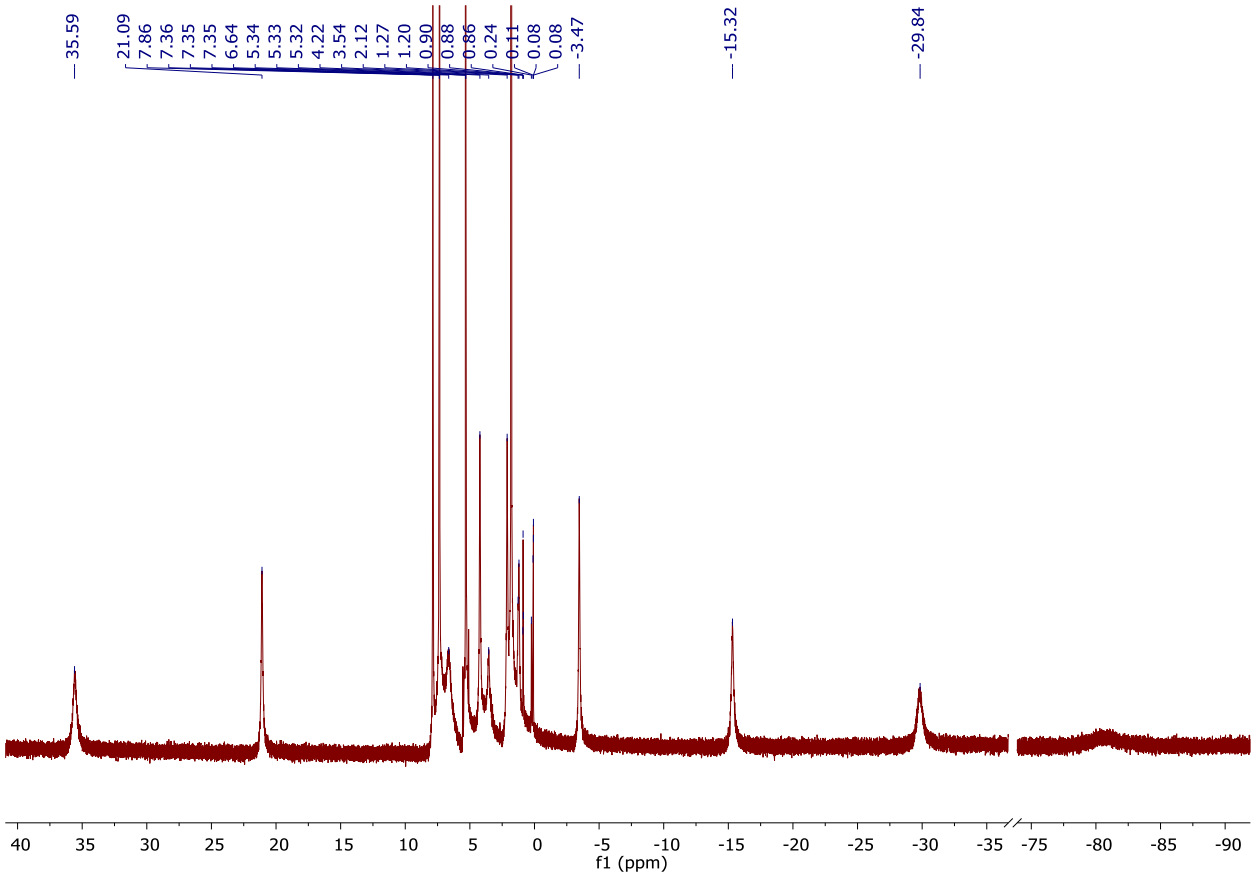

Figure S7. ^{1}H NMR (400 MHz) of **[Ni$_4$]$^{2+}$** in CD_2Cl_2.

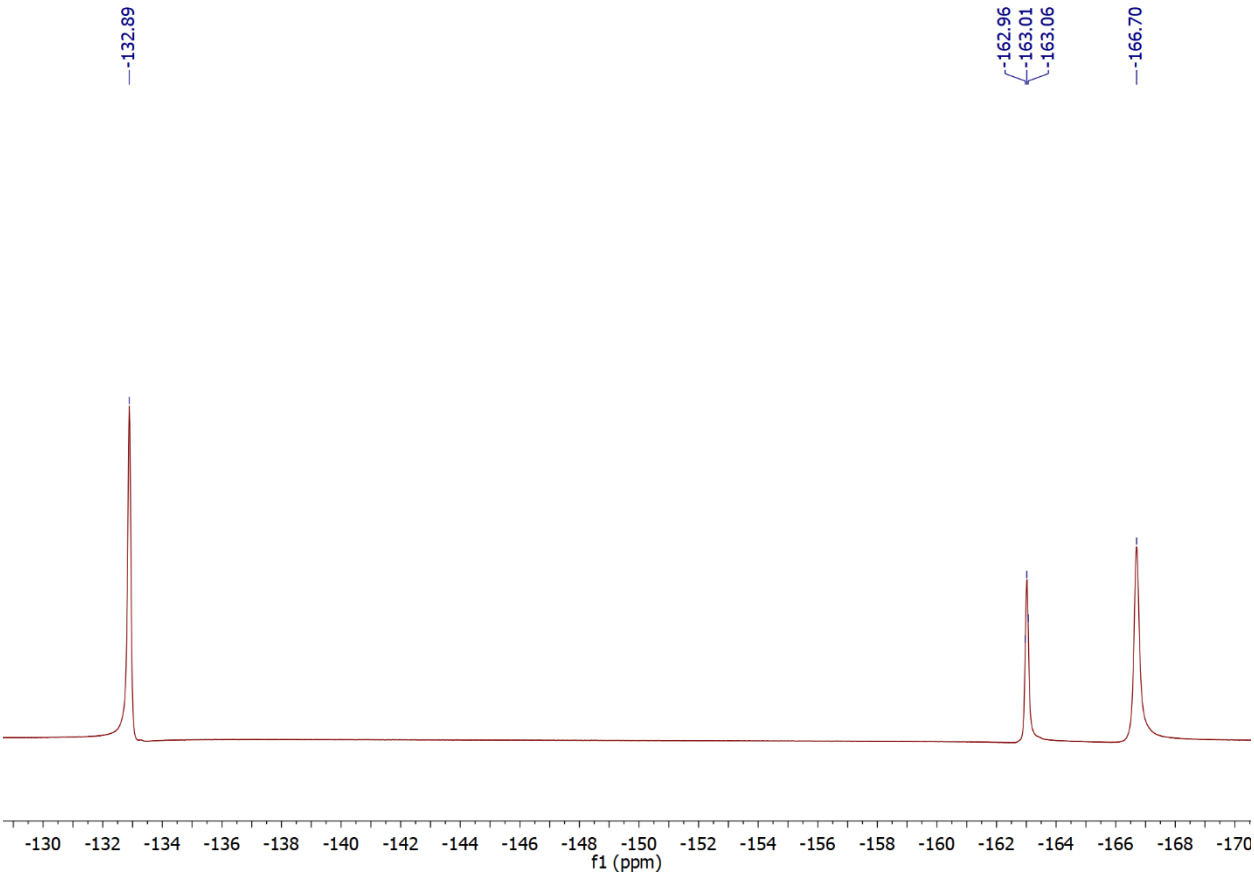

Figure S8. ^{19}F NMR (376 MHz) of **[Ni$_4$]**$^{2+}$ in CD_2Cl_2.

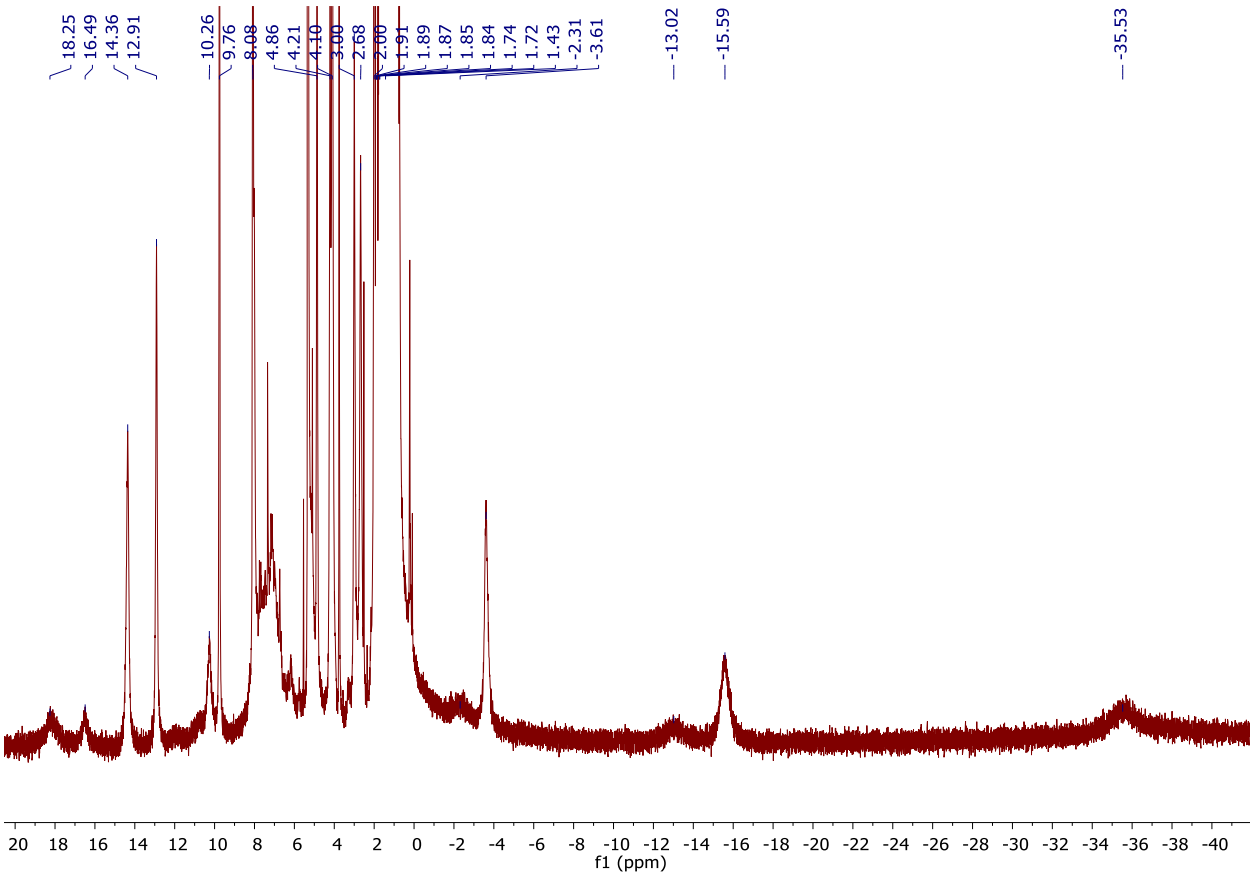

Figure S9. ^{1}H NMR (400 MHz) of **[Ni$_4$]$^{4+}$** in CD_2Cl_2 generated in situ by treating **[Ni$_4$]** to 10 equiv of [(2,4-$C_6H_3Br_2)_3N$][$B(C_6F_5)_4$].

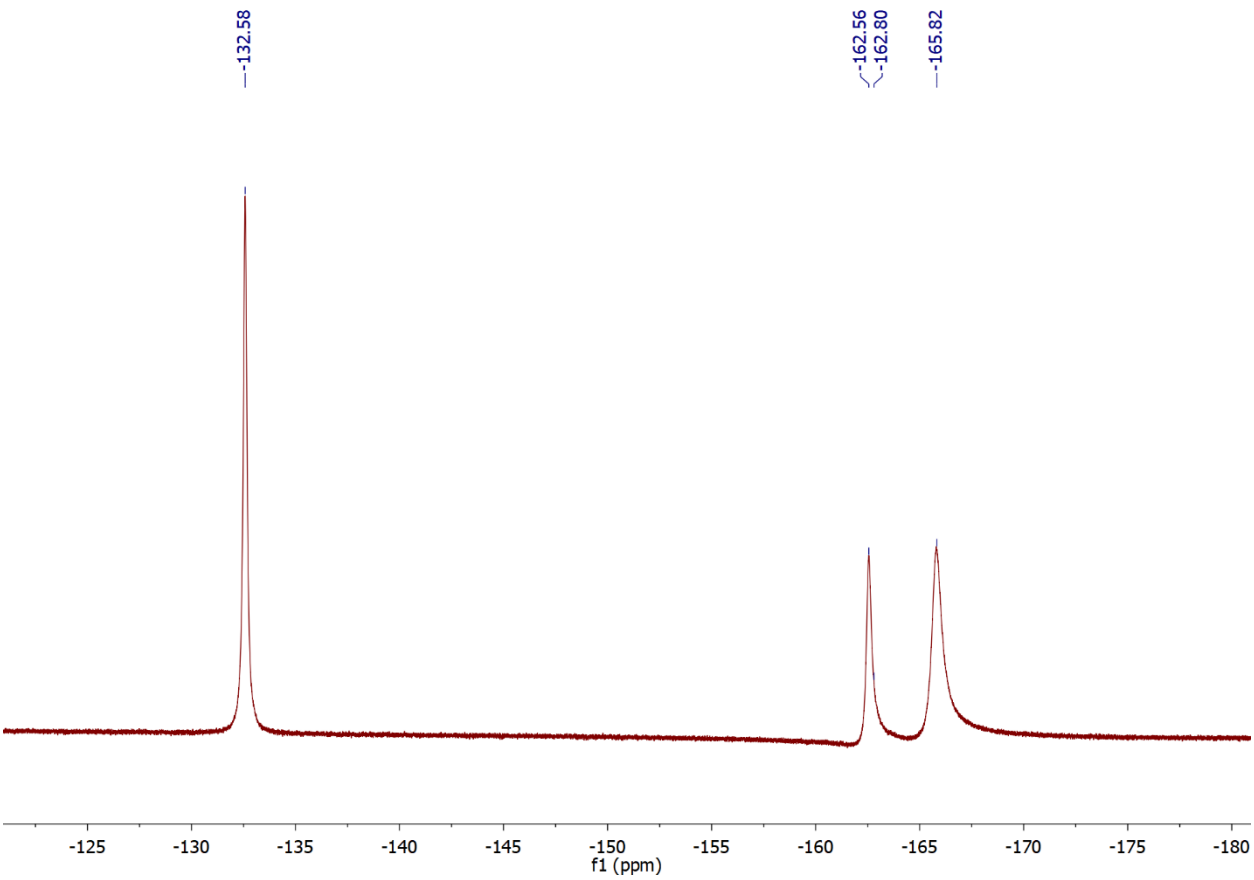

Figure S10. ^{19}F NMR (376 MHz) of **[Ni$_4$]$^{4+}$** in CD_2Cl_2.

4) UV-Vis Spectroscopy

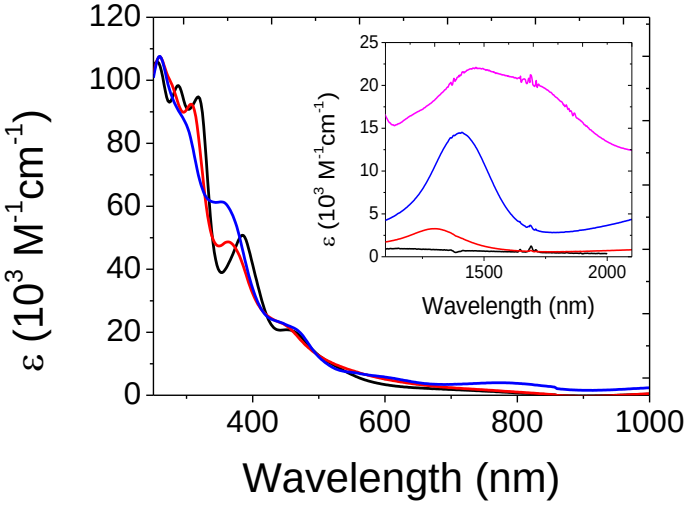

Figure S11. UV-visible spectrum of **[Ni$_4$]** (0.068 mM, black trace), **[Ni$_4$]$^+$** (0.088 mM, red trace), **[Ni$_4$]$^{2+}$** (0.089 mM, blue trace) in DCM. Inset: NIR spectrum of **[Ni$_4$]** (0.115 mM, black trace), **[Ni$_4$]$^+$** (0.396 mM, red trace), **[Ni$_4$]$^{2+}$** (0.216 mM, blue trace), and *in-situ* generated **[Ni$_4$]$^{4+}$** (0.426 mM, pink trace) in DCM. The **[Ni$_4$]$^{4+}$** complex was generated by treating **[Ni$_4$]** to 10 equiv of [(2,4-$C_6H_3Br_2)_3N$][$B(C_6F_5)_4$]. The **[Ni$_4$]$^{4+}$** UV-Vis is omitted due to the strong absorptions of the oxidant ([(2,4-$C_6H_3Br_2)_3N$][$B(C_6F_5)_4$]) saturating the detector.

5) EPR Spectroscopy

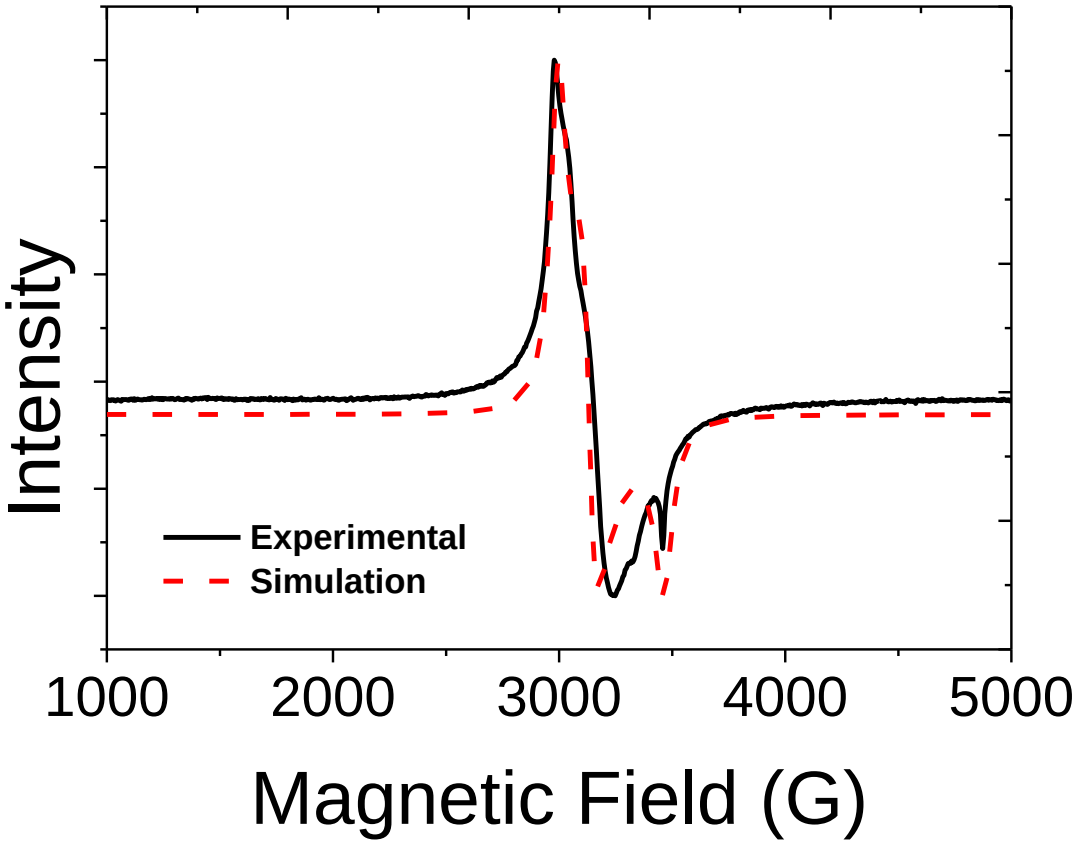

Figure S12. Experimental (black trace) and simulated (red trace) EPR spectrum of **[Ni$_4$]$^+$** in DCM at 100 K. The simulation yielded the following g-values: g_x = 2.01, g_y = 2.22, g_z = 2.32, and g_{av}= 2.18.

6) Magnetometry

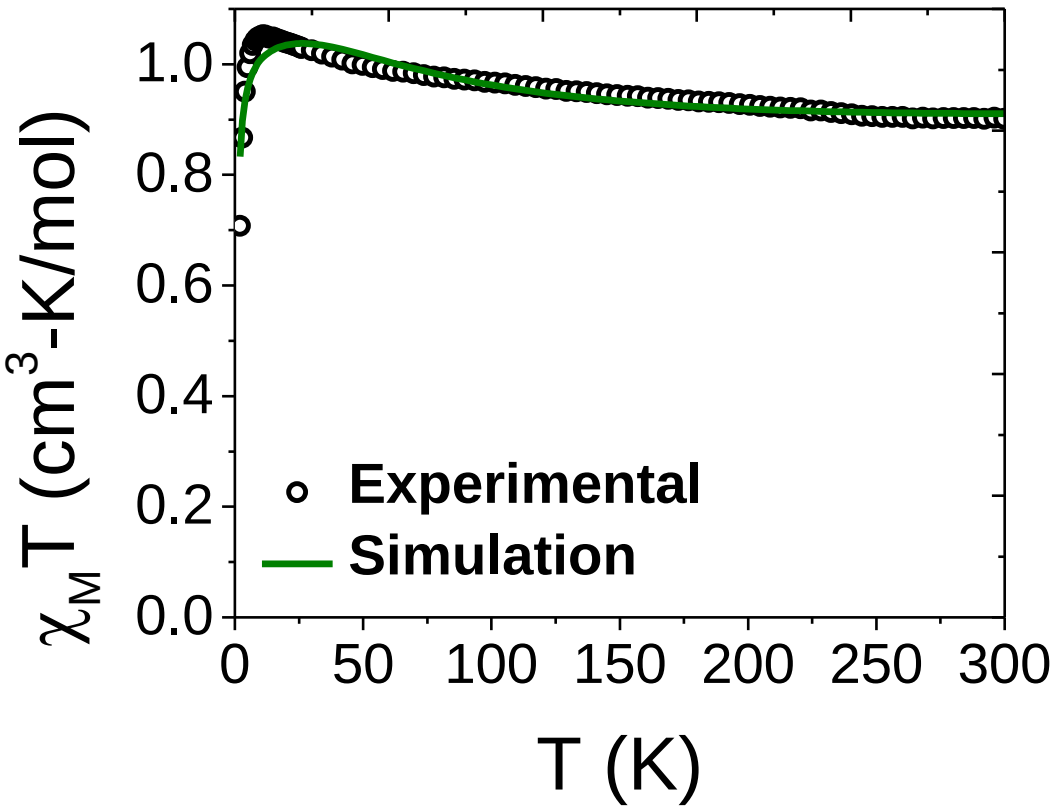

Figure S13. Molar magnetic susceptibility ($\chi_M T$) versus T measurements for bulk crystalline **$[Ni_4]^{2+}$** collected from 2 to 300 K (black circles) under a static 0.1 T field. The green trace represents the simulated fit with parameters: *g*-value = 2.06; J_{12} = 36.2 cm^{-1}, D = 2.16 cm^{-1}, E = 0.70 cm^{-1}, TIP = 177x10^{-6} $cm^{-3}mol^{-1}$, and zJ = -0.135 cm^{-1}.

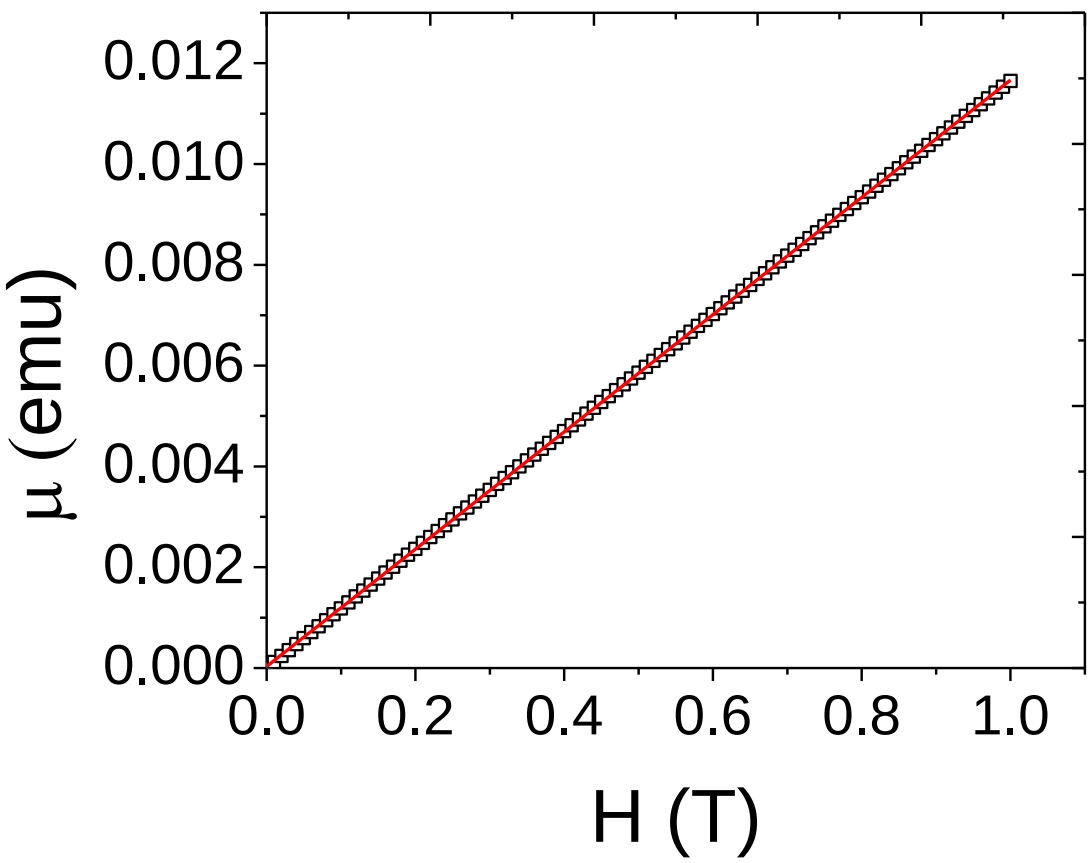

Figure S14. Magnetic moment vs magnetic field at 10 K for $[Ni_4]^{2+}$ used to check for ferromagnetic impurities.

7) Crystallography and Bond Measurements

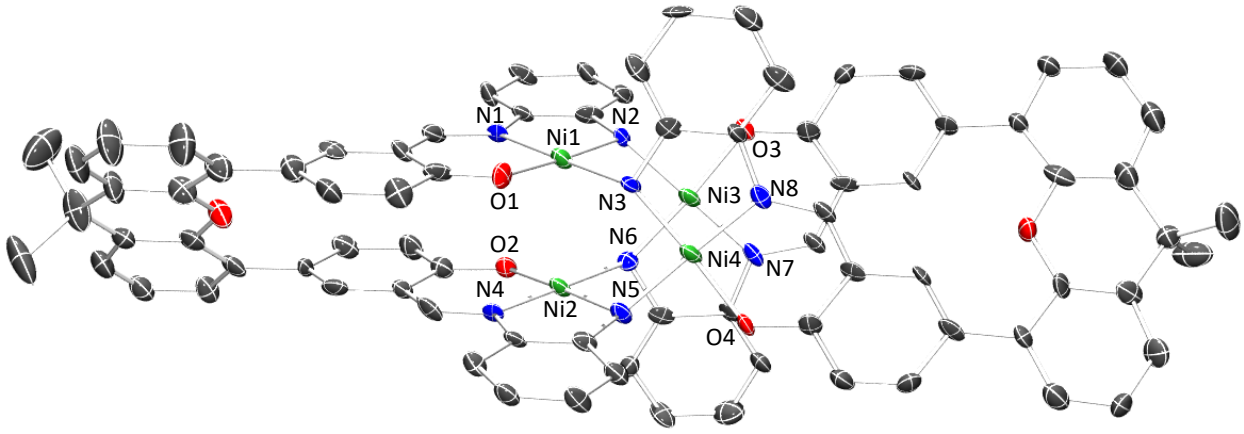

Figure S15. Solid state molecular structure of **[Ni$_4$]**. Hydrogen atoms and co-crystallized solvent molecules are removed for clarity (C, black; N, blue; O, red; Ni, green).

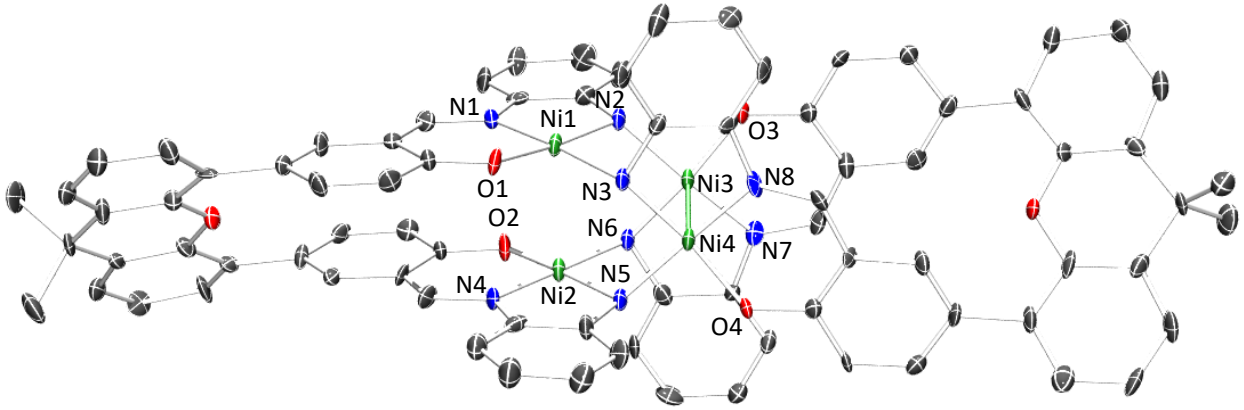

Figure S16. Solid state molecular structure of **[Ni$_4$]$^+$**. Solid green bond represents long Ni–Ni bond. Hydrogen atoms, PF_6 counteranion, and co-crystallized solvent molecules are removed for clarity(C, black; N, blue; O, red; Ni, green).

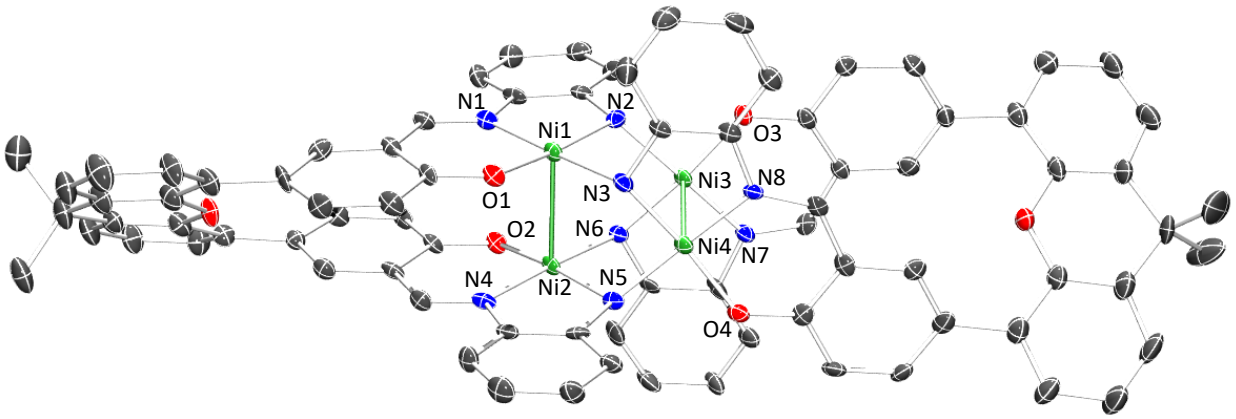

Figure S17. Solid state molecular structure of $[Ni_4]^{2+}$. Solid green bond represents long Ni–Ni bond. Hydrogen atoms, two $B(C_6F_5)_4$ counteranions, and co-crystallized solvent molecules are removed for clarity (C, black; N, blue; O, red; Ni, green).

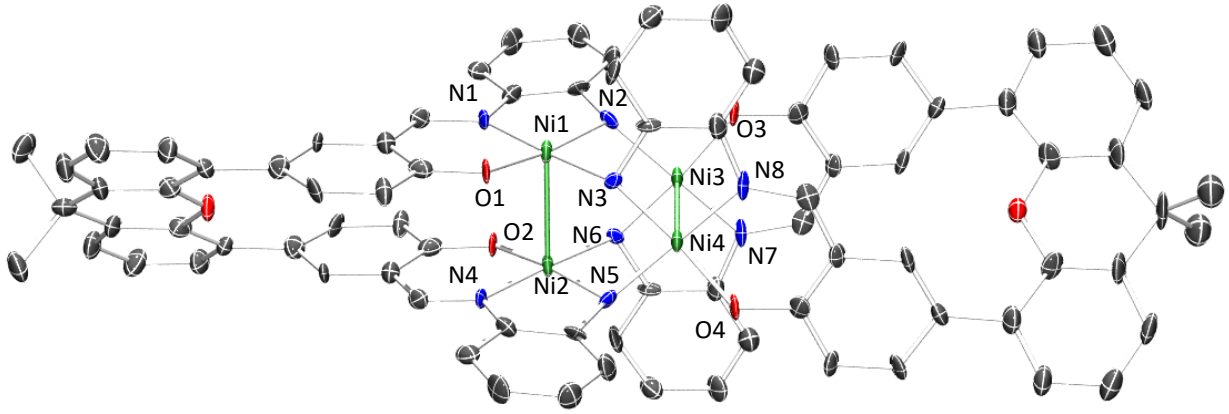

Figure S18. Solid state molecular structure of $[Ni_4]^{4+}$. Solid green bond represents long Ni–Ni bond. Hydrogen atoms, four $B(C_6F_5)_4$ counteranions, and co-crystallized solvent molecules are removed for clarity (C, black; N, blue; O, red; Ni, green).

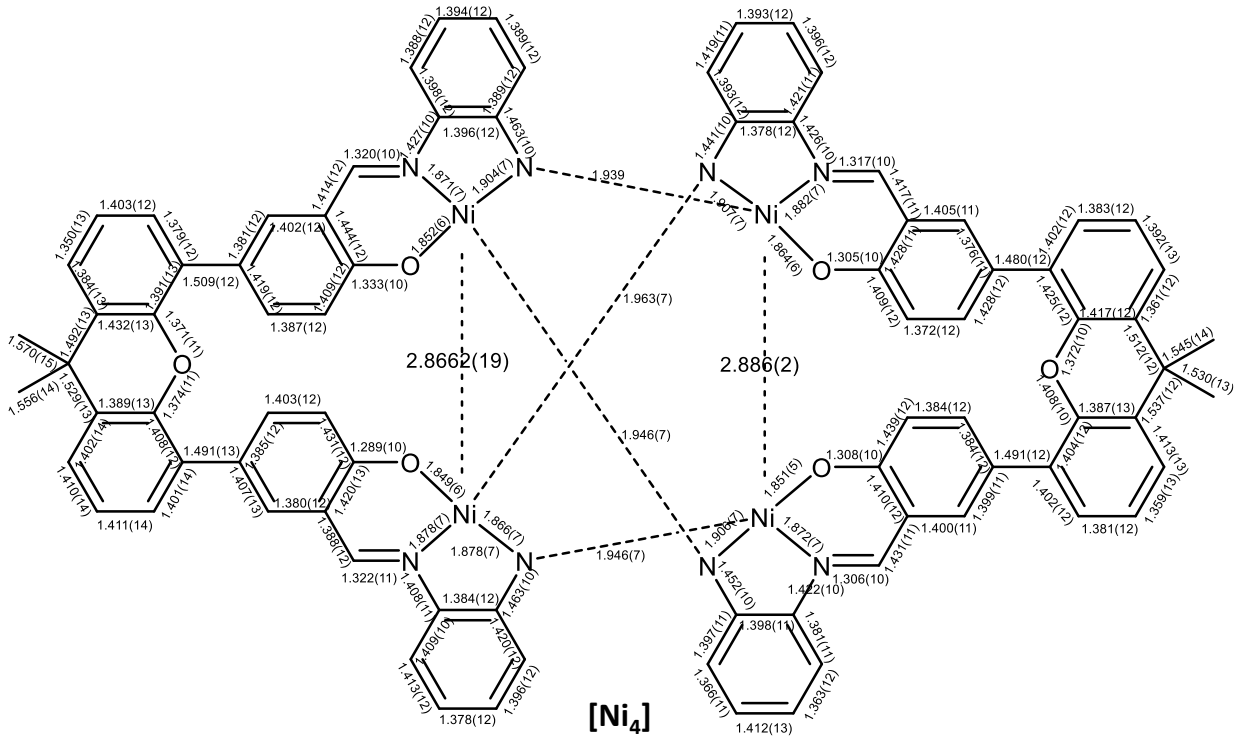

Figure S19. Bond lengths for complex **[Ni₄]**.

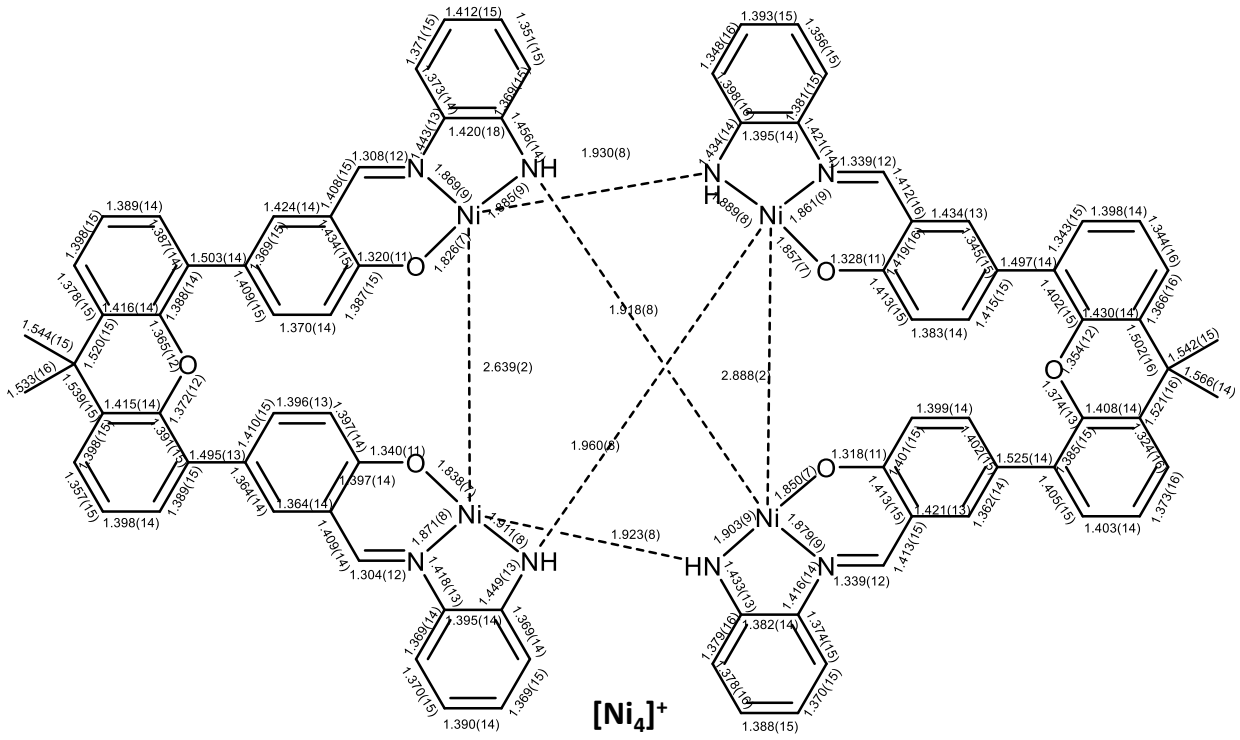

Figure S20. Bond lengths for complex **[Ni₄]⁺**.

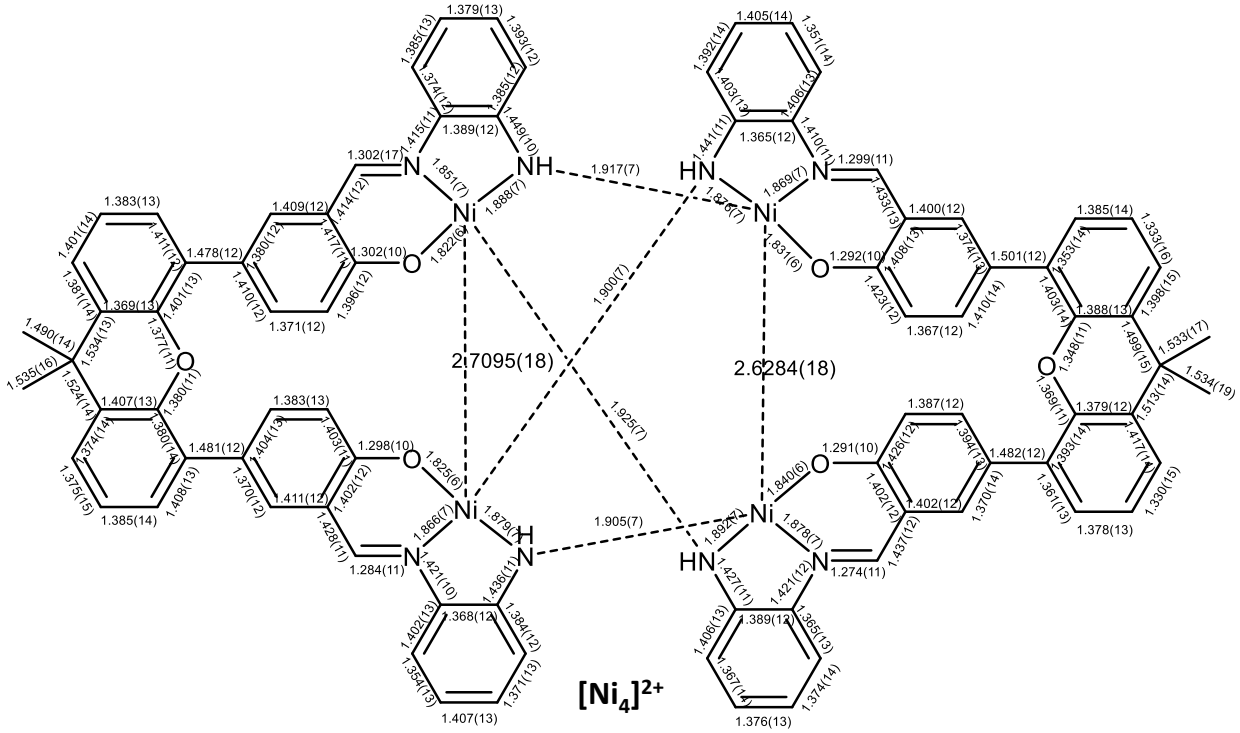

Figure S21. Bond lengths for complex $[Ni_4]^{2+}$.

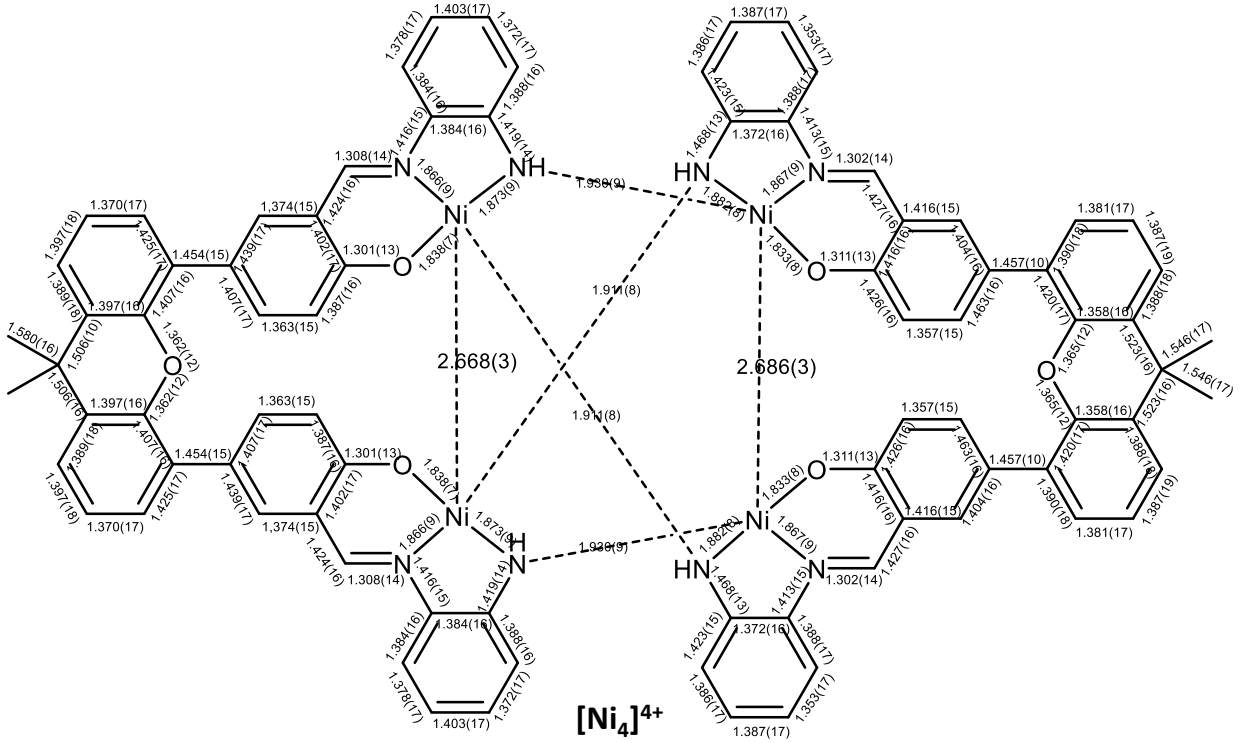

Figure S22. Bond lengths for complex $[Ni_4]^{4+}$.

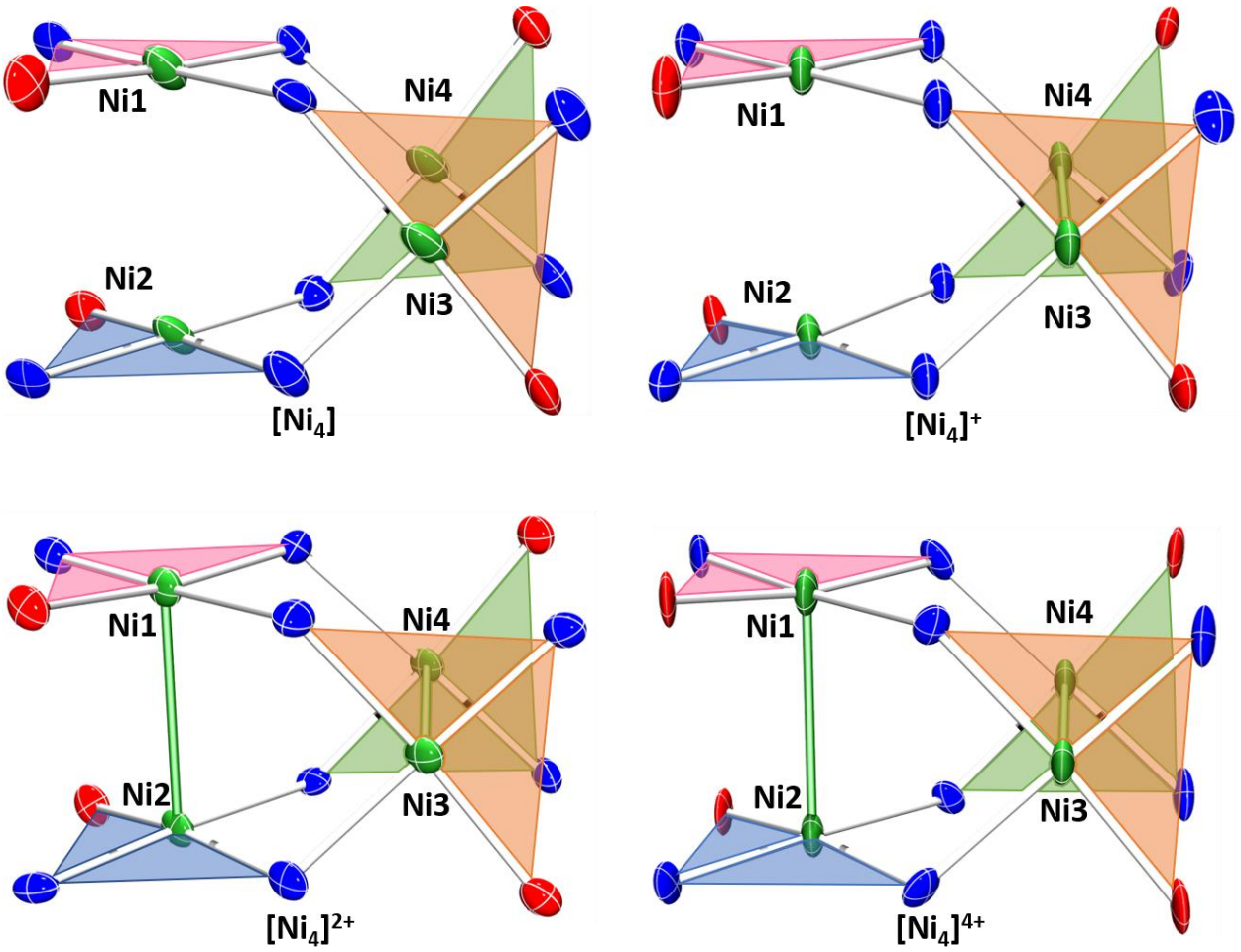

Figure S23. Drawn-in ligand planes for **[Ni$_4$]**, **[Ni$_4$]$^+$**, **[Ni$_4$]$^{2+}$**, and **[Ni$_4$]$^{4+}$** tetranuclear cores.

Table S1. Average bond lengths of immediate redox active ligand sites and Ni coordination sphere.

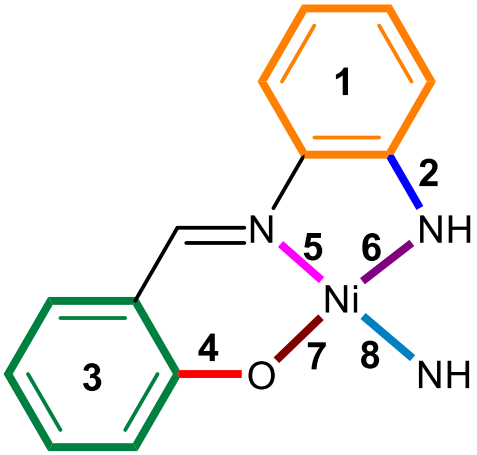

Nickel Complexes	Average Bond Lengths (Å)							
	Site 1	Site 2	Site 3	Site 4	Site 5	Site 6	Site 7	Site 8
$[Ni_4]$	1.395	1.455	1.404	1.309	1.876	1.896	1.854	1.949
$[Ni_4]^{+}$	1.379	1.436	1.397	1.328	1.867	1.890	1.841	1.926
$[Ni_4]^{2+}$	1.383	1.438	1.438	1.296	1.866	1.884	1.830	1.912
$[Ni_4]^{4+}$	1.385	1.444	1.405	1.307	1.867	1.878	1.836	1.921

8) Computational Details

All calculations were carried out at the DFT level of theory using the hybrid functional B3PW91[6,7] with the Gaussian 09[8] suite of programs. The Ni atom was represented with a Stuttgart-Dresden relativistic effective core potential associated with its adapted basis set.[9-11] All other atoms (C, H, O, N) were described with a 6-31G (d,p), double –ζ quality basis set. Geometry optimizations were computed without any symmetry constraints. The enthalpy energy was computed at T = 298 K in the gas phase. Natural Bonding Orbital (NBO) analyses were also conducted.[12,13]

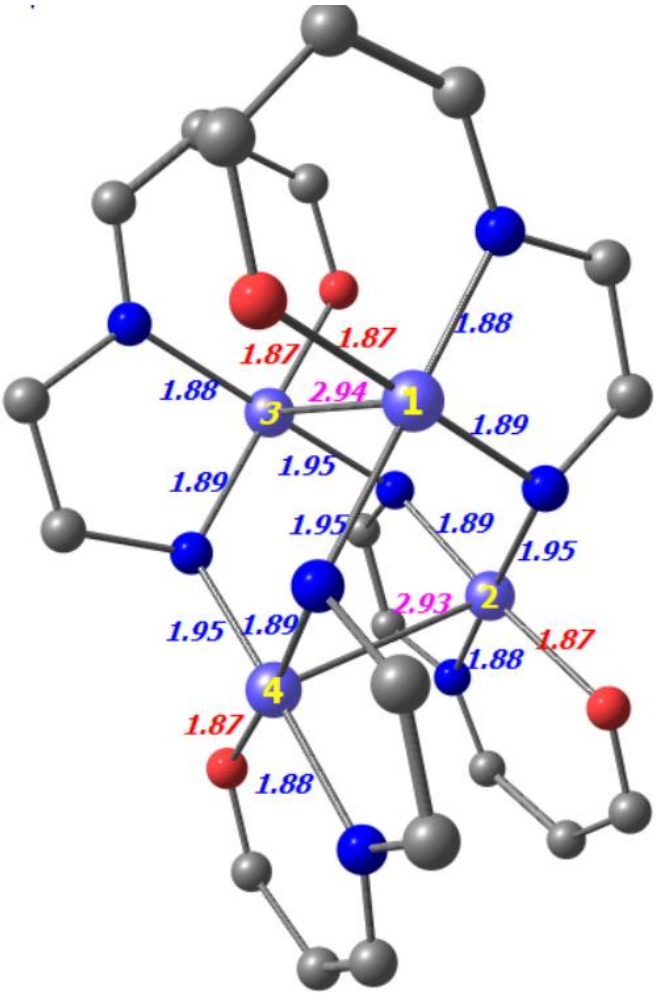

Figure S24: Optimized structure of the [Ni_4] neutral species

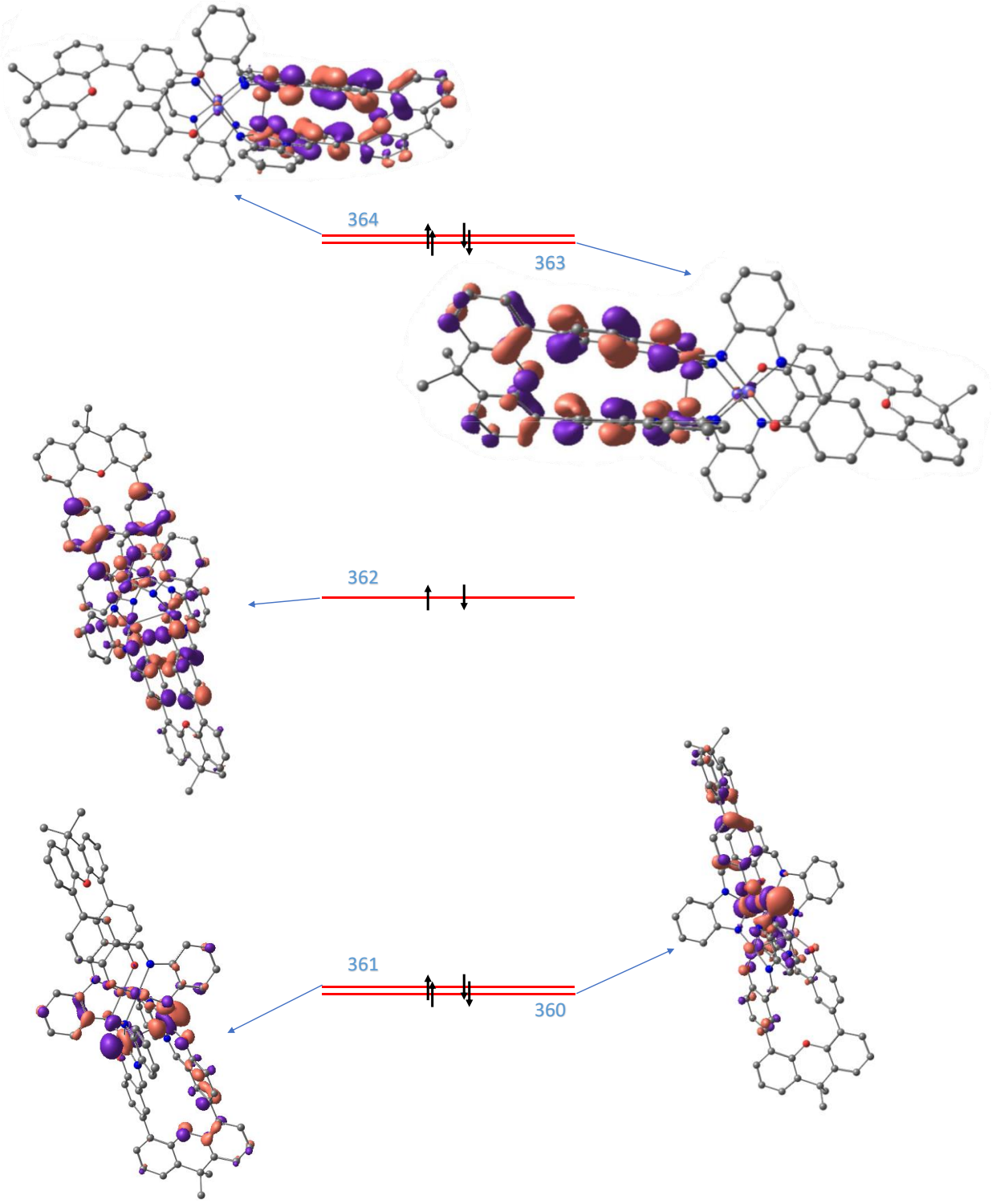

Figure S25: Simplified Frontier orbital diagram of the [Ni_4] complex.

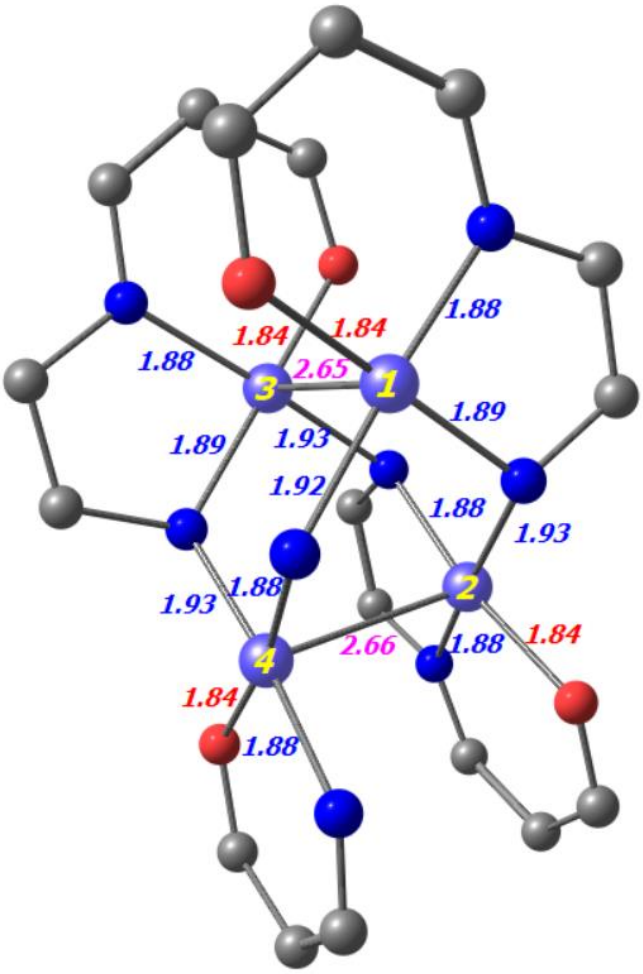

Figure S26: Optimized structure of the $[Ni_4]^{4+}$ species.

Cartesian coordinates of optimized structures

[Ni_4]

Ni	3.413943	9.333280	8.076387
Ni	4.471023	11.982202	6.344969
Ni	2.844028	11.959656	9.258026
Ni	1.597106	11.416190	6.208428
O	2.096371	8.401565	9.017598
O	4.889041	11.227208	4.687857
O	1.079285	13.131964	5.685384
O	4.245876	11.937857	10.493109
O	3.385296	7.846236	15.045347
N	1.432851	12.132522	8.011788
N	1.697742	10.738994	4.456331
O	2.770107	14.527033	-0.092235
N	1.982689	9.662915	6.799749
N	4.784295	8.951176	9.306428
N	4.274662	13.730287	5.677325
N	4.735031	10.174443	7.015651
N	4.183266	12.713684	8.062382
N	1.567870	11.273843	10.457508
C	3.079798	10.915074	12.330397
C	0.264573	11.232050	9.910841
C	3.417023	7.184508	12.215595
H	4.353250	7.168837	12.766485
C	2.279860	6.633868	12.785661
C	7.266188	9.274553	9.563341
H	7.310289	8.814692	10.545507
C	3.406230	7.783079	10.937068
C	4.604346	13.733469	2.024969
H	4.376554	14.789569	1.909422

C	4.856510	12.963247	0.900609
C	4.046012	14.685357	6.694769
C	-0.898212	10.781038	10.550628
H	-0.864190	10.365219	11.552673
C	1.107340	13.424218	2.029445
H	1.299664	12.807296	1.156030
C	1.201074	12.823505	3.303402
C	2.072053	8.772470	5.688452
C	3.167844	10.384319	13.635652
H	2.269155	9.966757	14.081204
C	1.974393	9.352927	4.416253
C	4.240977	11.459485	11.699806
C	4.618700	13.193169	3.329085
C	1.531613	11.438729	3.369102
H	1.649441	10.938494	2.407663
C	0.678257	15.398945	0.528719
C	3.806257	14.326266	-0.963080
C	0.794187	14.764164	1.863632
C	8.419022	10.303404	7.702497
H	9.343076	10.640679	7.240390
C	6.020102	10.026010	7.618763
C	6.050468	9.413708	8.879750
C	4.056117	14.132623	7.983146
C	2.288368	5.985346	14.119065
C	8.442443	9.722739	8.974083
H	9.383405	9.611734	9.506233
C	0.977248	13.603359	4.480245
C	0.546432	15.520475	3.035252
H	0.303199	16.576394	2.934586
C	7.212381	10.458324	7.027697

H	7.175012	10.914705	6.042397
C	4.862526	13.528345	-0.470486
C	2.863161	5.992238	16.512757
C	3.949737	8.551919	16.073135
C	4.892453	11.803879	3.524855
C	-2.121939	10.873208	9.897973
H	-3.021931	10.524228	10.397133
C	2.106932	8.557759	3.269524
H	2.049064	8.989385	2.275322
C	3.864680	16.064651	6.523695
H	3.838030	16.510467	5.534448
C	5.173342	11.031201	2.367930
H	5.385389	9.975021	2.507515
C	2.257185	7.390949	5.809532
H	2.313281	6.953578	6.802484
C	5.153241	11.593920	1.108390
H	5.349446	10.963612	0.243278
C	-1.044187	11.850685	7.967715
H	-1.083691	12.269075	6.965826
C	1.679480	15.267846	-0.458889
C	0.195129	11.746802	8.608647
C	3.806532	14.853613	-2.256341
C	3.933855	14.968201	9.098760
H	3.962298	14.526772	10.090994
C	1.088082	6.676614	12.020996
H	0.177873	6.259060	12.446852
C	-2.198402	11.418495	8.612785
H	-3.159550	11.500150	8.112065
C	1.815777	10.874152	11.673471
H	0.994520	10.465892	12.262738

C	2.370908	6.602560	4.669037
H	2.515298	5.529798	4.766677
C	0.631661	14.967542	4.296190
H	0.454894	15.566717	5.184880
C	4.343751	14.067945	4.420146
H	4.182189	15.112801	4.153996
C	4.625858	8.328919	10.441182
H	5.493850	8.202107	11.088450
C	1.698053	4.730262	14.290011
H	1.267417	4.235753	13.423055
C	5.951627	13.764548	-2.630896
H	6.791852	13.551034	-3.285871
C	2.858276	6.600768	15.255766
C	1.040276	7.254358	10.769249
H	0.113409	7.294364	10.204251
C	1.681424	4.102825	15.532872
H	1.225845	3.122783	15.644764
C	4.046139	8.035698	17.367253
C	4.354864	10.369172	14.350917
C	4.451627	9.826154	15.727355
C	2.192341	7.841927	10.184693
C	5.444448	11.461475	12.452094
H	6.331807	11.874701	11.981125
C	2.308086	7.188776	3.401296
H	2.409173	6.574818	2.510373
C	3.725041	16.883234	7.638297
H	3.586285	17.952475	7.502649
C	-0.437096	16.182183	0.220724
H	-1.223310	16.282578	0.964641
C	1.577094	15.873536	-1.713099

C	2.264999	4.730738	16.625493
H	2.258417	4.231097	17.590690
C	3.772595	16.338956	8.925342
H	3.676568	16.985213	9.793865
C	4.902346	14.557488	-3.077054
H	4.931954	14.957916	-4.087050
C	2.663040	15.722532	-2.775738
C	5.493514	10.934159	13.726005
H	6.440515	10.930351	14.262088
C	5.926759	13.257139	-1.334405
H	6.754304	12.655681	-0.967044
C	4.678133	8.826041	18.335615
H	4.765767	8.450891	19.351931
C	-0.563124	16.803603	-1.018999
H	-1.441383	17.402431	-1.244013
C	3.495712	6.659158	17.732100
C	2.050628	15.064862	-4.032990
H	1.230316	15.671300	-4.431974
H	2.798901	14.956621	-4.825686
H	1.656324	14.070685	-3.798686
C	0.434745	16.641871	-1.971267
H	0.327074	17.123558	-2.939611
C	5.079719	10.569136	16.730348
H	5.460315	11.557192	16.484365
C	4.648783	5.769425	18.249313
H	4.281787	4.775522	18.527786
H	5.418279	5.644924	17.480404
H	5.119880	6.210656	19.134535
C	3.216504	17.118276	-3.141073
H	3.995125	17.043178	-3.908055

H	2.424220	17.765056	-3.533792
H	3.650278	17.606116	-2.262101
C	5.196734	10.076989	18.027697
H	5.680829	10.672318	18.796976
C	2.429859	6.818765	18.839509
H	1.599899	7.442657	18.492172
H	2.023610	5.846405	19.138429
H	2.857890	7.287650	19.732142
H	4.988671	12.487737	8.653167
H	1.220441	9.352223	7.409181
H	4.750217	9.719965	6.098000
H	1.367327	13.115973	7.733819

$[Ni_4]^{4+}$

Ni	1.721880	11.471787	6.205525
Ni	2.892983	11.828231	9.224218
Ni	4.337454	11.947668	6.310282
Ni	3.364645	9.447990	8.154664
O	2.769203	14.557445	-0.171256
O	3.386682	7.807142	15.123414
O	4.244493	11.773677	10.470840
O	1.226492	13.151237	5.640079
O	4.741483	11.250807	4.655745
O	2.099995	8.528802	9.124952
N	1.549629	11.259402	10.414672
N	4.211665	12.620282	8.066492
N	4.644128	10.164047	6.968022
N	4.238951	13.732192	5.716234
N	4.798774	8.999174	9.289975
N	1.952292	9.725788	6.876968

N	1.725325	10.712403	4.481981
N	1.517942	12.183719	7.982920
C	2.390342	6.736731	18.866684
C	5.021316	10.136634	18.070092
C	3.148509	17.165047	-3.194323
C	4.687619	5.800229	18.334814
C	4.914003	10.624033	16.762672
C	0.377286	16.544903	-2.056582
C	2.108432	15.036722	-4.101224
C	3.497841	6.632622	17.783917
C	-0.632567	16.644602	-1.096114
C	4.561847	8.859173	18.400390
C	6.001586	13.416287	-1.267534
C	5.409911	10.869056	13.753076
C	2.661394	15.736543	-2.829950
C	4.965828	14.685469	-3.066930
C	3.880675	16.214920	9.084627
C	2.395416	4.650506	16.632262
C	1.548207	15.838161	-1.800103
C	-0.497719	16.032837	0.155294
C	3.824469	16.810800	7.820948
C	2.199454	7.099051	3.588693
C	5.397289	11.335764	12.456811
C	2.236840	7.921758	10.272345
C	4.329500	9.853732	15.763621
C	4.242328	10.354179	14.373632
C	3.986525	8.030464	17.441891
C	1.871396	4.020211	15.500488
C	1.095208	7.323939	10.857905
C	2.931979	6.546199	15.288464

C	6.033427	13.935573	-2.566748
C	1.876283	4.657681	14.254915
C	4.690321	8.328700	10.405819
C	4.361836	14.117474	4.474233
C	0.734286	14.947601	4.226984
C	2.258879	6.565693	4.879827
C	1.748621	10.905239	11.656173
C	-2.160187	11.647772	8.484132
C	1.181196	6.686041	12.075918
C	4.012625	14.834382	9.202433
C	3.837155	14.937000	-2.292789
C	0.240172	11.838247	8.541247
C	1.652288	15.225046	-0.533164
C	-0.970074	12.022234	7.867275
C	5.122486	11.694857	1.104774
C	2.177024	7.403993	5.987867
C	5.078141	11.100488	2.347050
C	3.918617	16.038949	6.668229
C	2.040857	8.466437	3.392886
C	-2.142404	11.089527	9.765896
C	4.790292	11.863523	3.504120
C	3.884928	8.551753	16.134419
C	2.934542	5.931186	16.558685
C	4.912771	13.651173	-0.435472
C	7.122894	10.432467	6.847692
C	0.588610	15.464548	2.958258
C	1.080348	13.588386	4.418793
C	8.443623	9.695520	8.735205
C	2.419825	5.929398	14.109927
C	4.090806	14.051443	8.047457

C	6.049451	9.431632	8.782610
C	5.965290	10.024470	7.515828
C	8.361111	10.265255	7.460958
C	0.796848	14.672418	1.799447
C	3.837436	14.408429	-0.984081
C	0.638565	15.294398	0.466118
C	1.510150	11.368555	3.373395
C	4.582371	13.268746	3.351077
C	4.201305	11.335847	11.699918
C	1.949911	9.313246	4.504291
C	3.056383	10.379456	13.651512
C	2.034465	8.781071	5.797546
C	1.237885	12.762865	3.263297
C	1.104319	13.329711	1.975641
C	-0.942910	10.918618	10.448142
C	4.062410	14.650786	6.781226
C	4.863649	13.078911	0.928398
C	4.612097	13.843160	2.060170
C	3.482940	7.816609	10.963194
C	7.296932	9.273591	9.398692
C	2.399678	6.617887	12.800450
C	3.532657	7.174633	12.221266
C	0.256292	11.303366	9.836141
C	3.005154	10.871323	12.327481
H	1.528791	13.184891	7.763020
H	4.592030	9.648267	6.083738
H	1.145242	9.492667	7.464287
H	5.060601	12.360358	8.578836
H	2.779667	7.221213	19.765271
H	2.042275	5.742633	19.156670

H	1.533102	7.312458	18.508280
H	5.459749	10.762689	18.841154
H	3.538398	17.690889	-2.318983
H	2.329493	17.753332	-3.614917
H	3.937649	17.117430	-3.948534
H	5.095811	6.264154	19.235939
H	5.489991	5.711837	17.597732
H	4.355895	4.795002	18.605595
H	5.262910	11.625437	16.530854
H	0.239013	17.032391	-3.015896
H	1.764176	14.022585	-3.882648
H	2.878357	14.981647	-4.874476
H	1.270879	15.604093	-4.514136
H	-1.537751	17.197460	-1.327809
H	4.661585	8.514351	19.424218
H	6.848359	12.849722	-0.893133
H	6.344293	10.872366	14.307967
H	5.024729	15.072687	-4.078690
H	3.825880	16.830470	9.976790
H	2.375639	4.125499	17.581508
H	-1.300876	16.109438	0.881475
H	3.719331	17.887591	7.734990
H	2.264349	6.440776	2.728242
H	6.300125	11.714987	11.989324
H	1.463409	3.017926	15.588032
H	0.154207	7.380343	10.320525
H	6.903262	13.761025	-3.192542
H	1.480033	4.143074	13.385210
H	5.600525	8.121410	10.966961
H	4.306955	15.184509	4.262652

H	0.583951	15.568000	5.104453
H	2.363140	5.494456	5.019269
H	0.882125	10.619472	12.251196
H	-3.104657	11.794052	7.969898
H	0.286488	6.243994	12.506113
H	4.068677	14.363099	10.178588
H	-0.974088	12.467712	6.877466
H	5.337252	11.082901	0.232762
H	2.208089	6.998938	6.994451
H	5.264305	10.038171	2.466463
H	3.890629	16.532542	5.702927
H	1.978790	8.846799	2.379168
H	-3.073126	10.797318	10.241573
H	7.049211	10.861492	5.853299
H	0.330913	16.513699	2.840446
H	9.411774	9.567963	9.208844
H	9.265240	10.573171	6.945591
H	1.522502	10.809661	2.438560
H	2.135373	10.032760	14.111499
H	1.228300	12.685320	1.109995
H	-0.963985	10.500889	11.448875
H	4.452190	14.913375	1.964878
H	7.395702	8.816745	10.377413
H	4.490428	7.102020	12.728493

9) References

1. M. Hirotsu, N. Ohno, T. Nakajima, C. Kushibe, K. Ueno and I. Kinoshita, *Dalton Trans.*, 2010, **39**, 139.
2. K. Lam and W. E. Geiger, *J. Org. Chem.*, 2013, **78**, 8020.
3. N. F. Chilton, R. P. Anderson, L. D. Turner, A. Soncini and K. S. Murray, *J. Comput. Chem.*, 2013, **34**, 1164.
4. D. F. Evans, *J. Chem. Soc.*, 1959, 2003.
5. G. A. Bain and J. F. Berry, *J. Chem. Educ.*, 2008, **85**, 532.
6. A. D. Becke, *J. Chem. Phys.*, 1993, **98**, 5648.
7. K. Burke, J. P. Perdew and Y. Wang, in *Electronic Density Functional Theory: Recent Progress and New Directions*, eds. J. F. Dobson, G. Vignale and M. P. Das, Plenum, New York, 1998.
8. *Gaussian 09, Revision D.01*, M. J. Frisch, G. W. Trucks, H. B. Schlegel, G. E. Scuseria, M. A. Robb, J. R. Cheeseman, G. Scalmani, V. Barone, B. Mennucci, G. A. Petersson, H. Nakatsuji, M. Caricato, X. Li, H. P. Hratchian, A. F. Izmaylov, J. Bloino, G. Zheng, J. L. Sonnengerg, M. Hada, M. Ehara, K. Toyota, R. Fukuda, J. Hasegawa, M. Ishida, T. Nakajima, Y. Honda, O. Kitao, H. Nakai, T. Vreven, J. A. Montgomery Jr, J. E. Peralta, F. Ogliaro, M. Bearpark, J. J. Heyd, E. Brothers, K. N. Kudin, V. N. Staroverov, T. Keith, R. Kobayashi, J. Normand, K. Raghavachari, A. Rendell, J. C. Burant, S. S. Iyengar, J. Tomasi, M. Cossi, N. Rega, N. J. Millam, M. Klene, J. E. Knox, J. B. Cross, V. Bakken, C. Adamo, J. Jaramillo, R. Gomperts, R. E. Stratmann, O. Yazyev, A. J. Austin, R. Cammi, C. Pomelli, J. W. Ochterski, R. L. Martin, K. Morokuma, V. G. Zakrzewski, G. A. Voth, P. Salvador, J. J. Dannenberg, S. Dapprich, A. D. Daniels, Ö. Farkas, J. B. Foresman, J. V. Ortiz, J. Cioslowski and D. J. Fox, Gaussian.
9. X. Cao and M. Dolg, *J. Mol. Struct. THEOCHEM*, 2004, **673**, 203.
10. W. Küchle, M. Dolg, H. Stoll and H. Preuss, *J. Chem. Phys.*, 1994, **100**, 7535.
11. X. Cao, M. Dolg and H. Stoll, *J. Chem. Phys.*, 2003, **118**, 487.
12. F. Weinhold, in *Encyclopedia of Computational Chemistry*, ed. P. v. R. Schleyer, JohnWiley & Sons, Chichester, 1998, p. 1972.
13. A. E. Reed, L. A. Curtiss and F. Weinhold, *Chem. Rev.*, 1988, **88**, 899.